Capsules and their traits shape phage susceptibility and plasmid conjugation efficiency

Matthieu Haudiquet[1,2*], *Amandine Nucci*[1], *Julie Le Bris*[1], *Rémy A. Bonnin*[3], *Pilar Domingo-Calap*[4], *Olaya Rendueles*[1†], *Eduardo P.C. Rocha*[1†]

[1] Institut Pasteur, Université Paris Cité, CNRS UMR3525, Microbial Evolutionary Genomics, Paris, 75015, France.

[2] Ecole Doctoral FIRE–Programme Bettencourt, CRI, Paris, France

[3] Team Resist UMR1184 Université Paris Saclay, CEA, Inserm, Le Kremlin-Bicêtre, France; Service de bactériologie, Hôpital Bicêtre, Université Paris Saclay, AP-HP, Le Kremlin-Bicêtre, France
Centre national de référence associé de la résistance aux antibiotiques, Le Kremlin-Bicêtre, France.

[4] Instituto de Biología Integrativa de Sistemas, Universitat de València-CSIC, 46980, Paterna, Spain

[*] Corresponding author: matthieu.haudiquet@gmail.com

[†] Equal contributions

Keywords: capsule, serotype, horizontal gene transfer, evolution, bacteriophages, antimicrobial resistance, plasmids, conjugation

Summary

Bacterial evolution is affected by mobile genetic elements such as phages and conjugative plasmids, which may provide novel adaptive traits but also incur in fitness costs. Infection by these elements is affected by the bacterial capsule. Yet, its importance has been difficult to quantify and characterise because of the high diversity of bacterial genomes regarding confounding mechanisms such as anti-viral systems. We swapped capsule loci between *Klebsiella pneumoniae* strains to quantify their effect on transfer of conjugative plasmids and phages independently of the genetic background. Capsule swaps systematically invert phage susceptibility, demonstrating that serotypes are key determinants of phage infection. Capsule types also affect conjugation efficiency in both donor and recipient cells depending on the serotype, a mechanism shaped by the capsule volume and depending on the structure of the conjugative pilus. Comparative genomics confirmed that more permissive serotypes in the lab correspond to the strains acquiring more conjugative plasmids in nature. The pili least sensitive to capsules (F-like) are also the most frequent in the species' plasmids, and are the only ones associated with both antibiotic resistance and virulence factors, driving the convergence between virulence and antibiotics resistance in the population. These results show how the traits of cellular envelopes define slow and fast lanes of infection by mobile genetic elements, with implications for population dynamics and horizontal gene transfer.

Graphical abstract

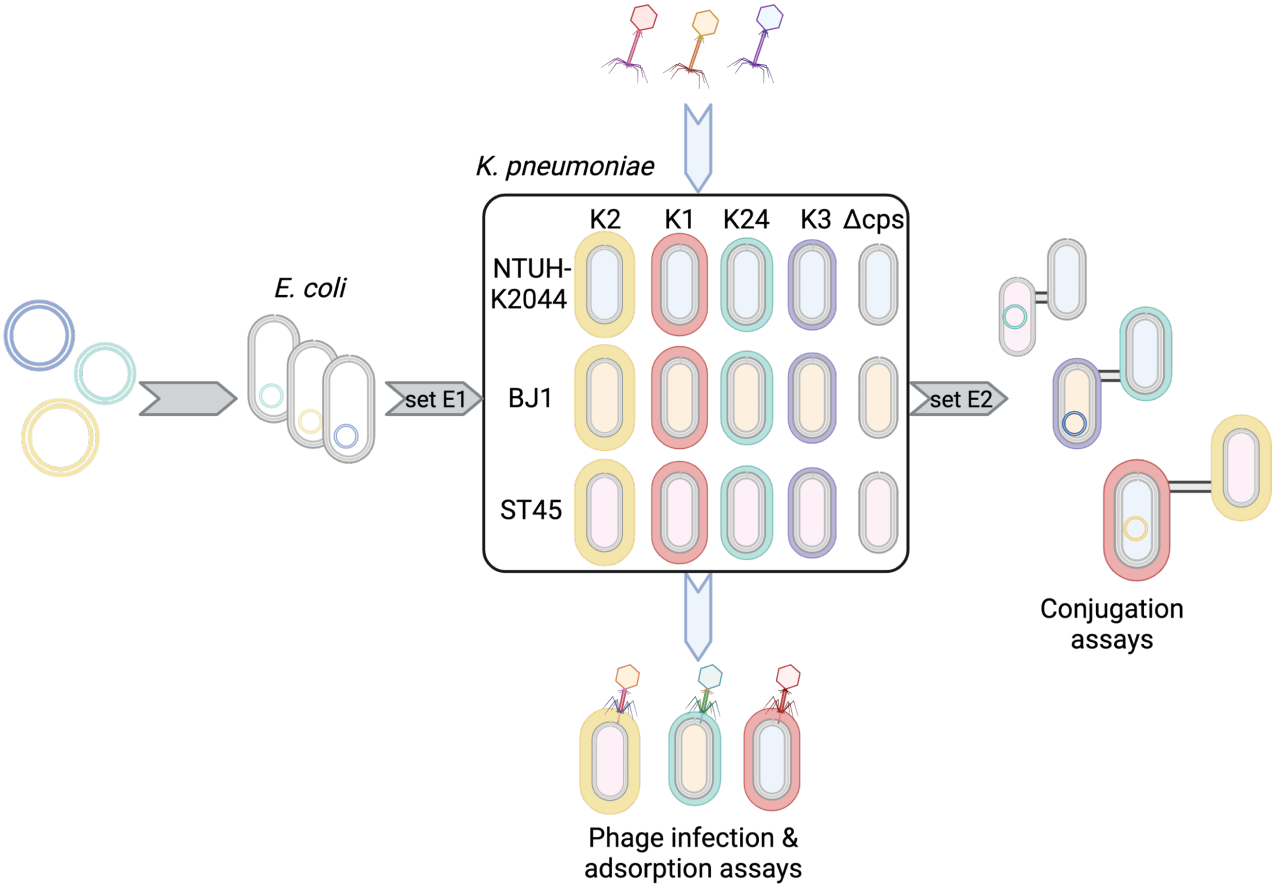

Introduction

Bacterial capsules are the outermost cellular structure. They protect from multiple challenges such as desiccation [1], bacteriophage (phage) predation [2,3] protozoan grazing[4], and the host's immune cells like macrophages [5,6]. Their ability to protect the cell may explain why they are an important virulence factor among all nosocomial species, including the ESKAPE pathogens *Enterococcus faecium*, *Staphylococcus aureus*, *Klebsiella pneumoniae*, *Acinetobacter baumannii*, *Pseudomonas aeruginosa*, and *Enterobacter spp.* [7]. Around half of the bacterial genomes encode at least one capsule [8], usually composed of thick, membrane-bound polysaccharide polymers surrounding the cell [9]. Group I capsules, also known as Wzx/Wzy-dependent capsules, are the most frequent ones [8]. Capsules in this group have similar assembly pathways but very diverse sets of enzymes which result in a large variety of capsule compositions, called capsule serotypes [10]. Their highly variable nature suggests that capsule composition is under some sort of balancing or diversifying selection [11]. Accordingly, capsule loci are frequently lost and acquired by horizontal gene transfer (HGT) [12,13].

Phage infections have an important impact on bacterial population dynamics [14,15]. They require an initial step of adsorption of the viral particle to the host's cell surface. Since the capsule covers the latter, phage-capsule interactions are key determinants of the success of phage infections. In many cases phages are blocked by the obstacle caused by the capsule and cannot reach their cell receptor [2,16]. Yet, some phages have evolved mechanisms to bypass the capsule barrier, such as encoding hydrolases called depolymerases which digest the capsule [17–22]. Such phages can recognize and attach to capsules of the serotype for which they encode a depolymerase. Hence, the phage-bacteria antagonistic co-evolutionary process has made these phages dependent on the bacterial capsule to adsorb efficiently to the cell. This explains why the capsule serotype shapes the host range of these phages [12,23,24]. In *Klebsiella pneumoniae* (*K. pneumoniae*), a species where most strains are heavily capsulated, the tropism of phages to one or a few serotypes results in an excess of successful infections between strains of the same serotype [12,23,24]. This could explain why selection for *K. pneumoniae* resistant to phages often results in mutants where the capsule was inactivated [22,25,26] or swapped to another serotype by HGT [12,27–29]. There is thus a complex interplay between bacteria and phages in species where most strains are capsulated: phages are blocked by the capsule, when it hides the cell surface and they lack appropriate depolymerases [6,18], or they depend on the presence of a capsule when they can adsorb and depolymerise it [29–31]. This interplay has implications for population dynamics, because the lytic cycle of most phages results in cell death. It also affects genetic exchanges because temperate phages can integrate the bacterial genome and provide novel traits by lysogenic conversion. Many phages also drive the horizontal transfer of bacterial DNA by transduction [32].

Conjugation is the other main mechanism of HGT driven by mobile genetic elements (MGEs) [33]. It has a key role in bacterial adaptation by mediating the transfer of many traits, from secondary metabolism to antibiotic resistance [34–36]. It relies on mating pair formation (MPF) systems that include a type IV secretion system. The latter were classed into eight distinct types based on gene content and evolutionary history [37]. The three most prevalent MPF types of plasmids in Proteobacteria are MPF_F (named after plasmid F), MPF_T (named after the Ti plasmid) and MPF_I

(named after the IncI R64 plasmid) [38]. While MPF_F conjugative pili are typically long (up to 20 µm) [39,40], flexible and retractable [41], MPF_T and MPF_I are shorter and rigid (<1 µm) [41–44]. Even though there is very little published information on the effect of capsules on conjugation, we showed recently that conjugation of one plasmid from a non-capsulated *Escherichia coli* strain to different *Klebsiella* strains was higher in Δ*wcaJ* mutants which do not produce capsules than in the capsulated wild type strains [12]. Similar effects of *wcaJ* inactivation were later found for one MPF_T plasmid [45] and bla_{KPC-2}-carrying plasmids of undetermined types [46]. However, the mechanism underlying these results remains unknown. Furthermore, conjugation rates might be more affected by certain serotypes or combinations of serotypes [47]. Computational studies failed to find an excess of conjugation between strains of the same serotype relative to pairs of strains with different ones [12], but whether some serotypes have systematic higher conjugation rates is unknown. Similarly, there is little information on how the presence of a capsule in the donor cell affects conjugation.

K. pneumoniae is a good model to study the effect of capsules on the transfer of MGEs. Indeed, most strains have one single genetic locus encoding a capsule which varies a lot in terms of volume and chemical composition between serotypes (of which more than 130 have been characterized computationally) [48–50]. *K. pneumoniae* is also an important nosocomial pathogen in which many virulence factors and antibiotic resistance genes are encoded in plasmids including carbapenemases and 16S rRNA methylases [51–54]. It is also a bacterial species with a large environmental breadth outside mammals [55,56]. *K. pneumoniae* genomes contain many prophages, which upon induction have been shown to produce temperate phages that are specific of one or a few serotypes [23]. It is also the focus of very productive lines of research to develop phage therapies to target multi-resistant strains [57]. The clinical characteristics of *K. pneumoniae* are associated with specific serotypes. Some clones are called hypervirulent because they provoke infections in healthy individuals including liver abscesses. They are almost exclusively of the K1 or K2 serotypes [58] and often produce very thick capsules that are thought to facilitate infection of humans [59]. Other examples include K3 strains which are associated with rhinoscleromatis, or K24 which are associated with nosocomial infections. Both K3 and K24 are often multi-drug resistant because they acquired multiple MGEs encoding antibiotic resistance genes [60,61]. Hence, virulence and resistance are associated with specific serotypes and both traits were gained by the acquisition of conjugative elements encoding them [62]. Yet, the interplay between capsules and conjugation and how this affects bacterial traits remains poorly understood.

Here, we sought to characterize the influence of capsule serotypes on the infection of *K. pneumoniae* cells by phages and conjugative plasmids. As mentioned above, previous works showed that phage host range depends on the capsule serotype [12,17,25,63] whereas plasmid acquisition might be facilitated by the loss of the capsule [12,45,46]. Yet, it has remained difficult to isolate the impact of these effects because strains with similar serotypes also tend to be more genetically related. A precise understanding of the interplay between capsules and MGEs needs a control for variation of strains' genetic background because the success and rates of infections also depend on the cell physiology (e.g., growth rate), the presence of defence systems (e.g., restriction-modification), the envelope composition (e.g., LPS), and genetic interactions between the MGE and the genome (e.g. repression of incoming phages by resident prophages) [64,65]. To solve this deadlock, we swapped capsular loci among strains. This is challenging because capsule swapping requires to build complex isogenic

mutants, *i.e.* precisely exchanging ~30kb capsule loci between strains. We devised a scalable method to generate such *K. pneumoniae* serotype swaps and used it to study phage and plasmid infection in strains with different serotypes in isogenic backgrounds. These mutants allowed to show that serotype swaps lead to the expected swap of phage host range. We then leveraged a diverse set of clinically-relevant plasmids to confirm the importance of the capsule in shaping conjugation efficiency in the recipient cell. The control for the genetic background allowed us to show that capsules also affect conjugation efficiencies for the donor cell and that some serotypes are associated with higher rates of transfer. To shed light on the mechanisms explaining these results we quantified the effective volume of individual cells in bacterial colonies to test whether the volume of the capsule affects conjugation efficiency. Finally, we used comparative genomics to test if these results contribute to explain the distribution of plasmids in hundreds of complete genomes of *K. pneumoniae*. Indeed, the frequency of the different types of plasmids and the number of plasmids recently acquired per serotype match the expectations given by the experimental data.

Results

Serotype swap shifts phage sensitivity and resistance.

To test the precise influence of the capsule and its different serotypes on infection by MGEs, we first deleted the complete capsule locus (Δ*cps*) and confirmed that the mutants were non-capsulated (Figure S1). We focused on a set of three strains recently isolated, belonging to three different sequence types (ST), namely NTUH (ST23), BJ1 (ST380), and an ST45 isolate (see Table S1 *Strains*). We then used these strains as chassis to insert the four selected serotypes (serotypes K1, K2, K3 and K24 (Figure 1A) via a novel scarless method (See *Construction of mutants*). These serotypes were chosen for their clinical relevance (see above) and because the genetics and the chemical composition of their capsules are well-known [48]. All mutants were verified by whole-genome sequencing (See *Mutants and transconjugants validation*). These null and swapped mutants will allow us to assess the interplay between MGEs, capsules (and their serotypes) while controlling for the host genetic background.

In parallel, we generated lysates from three virulent phages, each able to replicate in only one of the three wildtype strains. For clarity, we refer to those phages according to the capsule serotype of their original host: phK1, phK2 and phK24. As expected, the Δ*cps* mutants were resistant to all three phages, indicating that all phages required the presence of a capsule for infection (Figure 1B). We then enquired if the host sensitivity to phages is also lost when the serotype is swapped. We challenged the mutants having swapped capsular loci with the phages. We found that all those chassis strains that were susceptible to the phages became resistant upon change of the serotype (Figure 1B) showing that, capsule inactivation or swapping are sufficient to make bacteria resistant to phages for which they were originally sensitive.

If capsule serotypes are the key determinants of phage host range, then when the capsule serotype is swapped one should observe an inversion of sensitivity. We tested if the acquisition of a novel serotype led to gain of sensitivity to the cognate phage. Indeed, in four out of six cases the serotype swap resulted in the emergence of sensitivity to phages to which the wildtype strain was resistant (Figure 1B, S2). To understand the two cases (BJ1::K1+phK1 and NTUH::K2+phK2) not resulting in productive infections, we performed adsorption assays and observed significant adsorption at the cell surface for both pairs, in the same proportion as for susceptible hosts (Figure S3) proving that these phages can adsorb to the cell when the latter expresses the cognate capsule. We considered two hypotheses for why infection is subsequently hampered in these cases. First, the phages could depend on a secondary receptor. We find this hypothesis unlikely given that Δcps mutants of susceptible hosts were resistant. Second, anti-phage systems in the hosts could interfere with phage infection after adsorption. To enquire on this possibility, we analysed the genomes of the three strains with DefenseFinder [66,67] and found that each strain encoded four to eight known defence systems with no homologs in the other strains (Figure 1B). This may explain why certain bacteria are resistant to phage even when they acquired a capsule to which the phage adsorbs. It also fits previous analyses in other species where infection results from success at two key steps: adsorption at the cell envelope and resistance to anti-phage systems within the cell [68]. Given that these results clearly demonstrate

the effect of capsule swaps in gaining the ability to adsorb the novel phages and given the large number of defence systems identified, we have not engaged further in the analysis of the latter. Overall, these results show that serotype swaps result in the inversion of the patterns of sensitivity to phages, even if sometimes gaining a novel capsular locus does not allow productive phage infection.

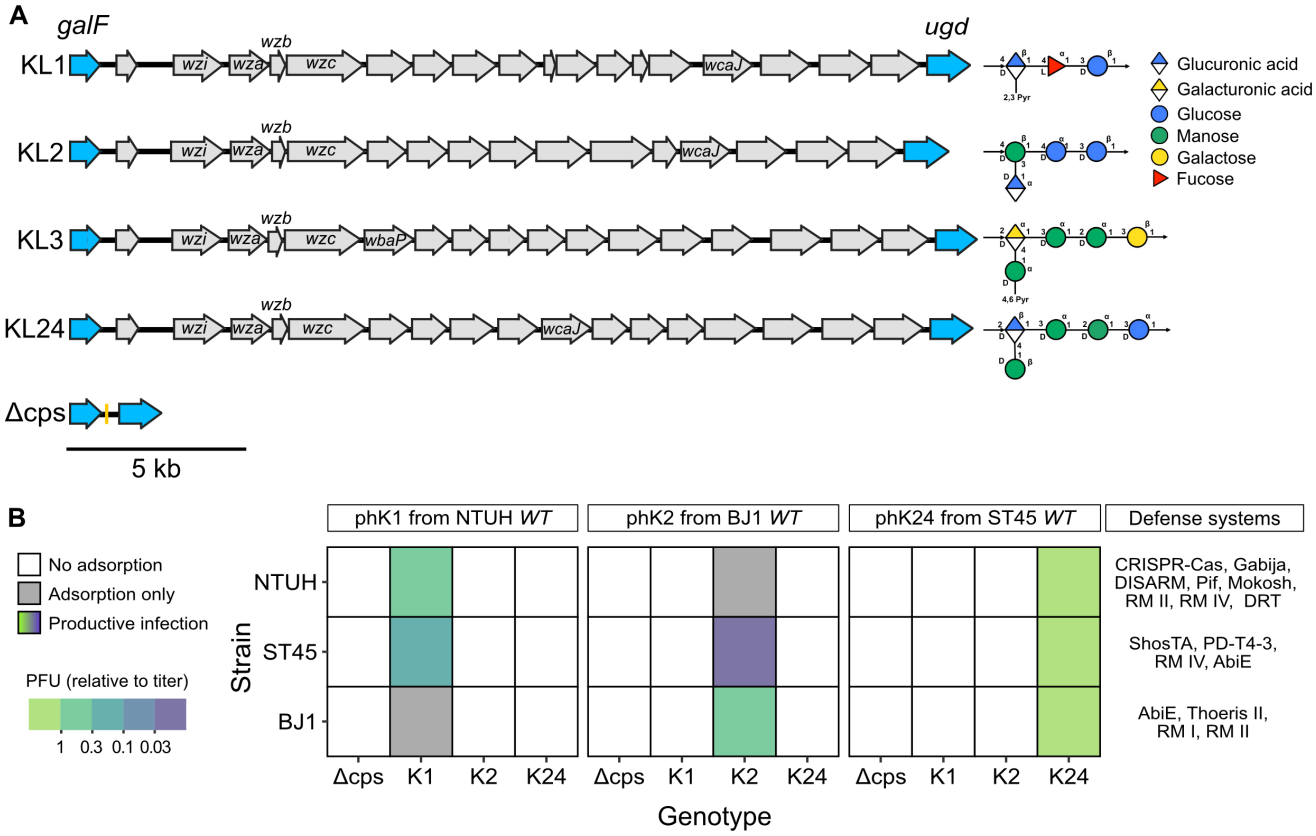

Figure 1 –A. Overview of the genetic loci encoding the four different capsule serotypes included in this study and their chemical composition. Arrows represent the different genes, *galF* and *ugd* in blue corresponding to the regions involved in homologous recombination to generate the swaps. Conserved genes involved in assembly and export of the capsule (*wza*, *wzb*, *wzc*, *wzi*) and initiating glycosyl-transferase (*wcaJ*, *wbaP*) are labelled. The chemical composition of the capsule (monomers and their organisation), is displayed on the right of each locus (predicted by K-PAM [69]). **B. Matrix of phage infection.** Infection assay for each of the three phages (panels), three swapped strains (y-axis), and different genotypes (x-axis). White tiles correspond to non-productive infection, *i.e.* no plaque could be identified. Coloured tiles correspond to the average PFU/mL normalized by the lysate titre for productive infections (Figure S2). Grey tiles correspond to non-productive infection with significant adsorption, while white tiles correspond to non-adsorptive pairs (Figure S3). Values are the average of three independent replicates. Strain-specific defence systems identified by DefenseFinder as of 02/2023 [70] are displayed on the right. Associated data are available as Supplementary Dataset S1 (Adsorption) and S2 (Infection).

The serotype of the recipient influences conjugation

To identify the effects of the capsule (and its serotype) in the cell's ability to receive conjugative plasmids while controlling for the genetic background, we assembled and sequenced a collection of 10 diverse conjugative plasmids from clinical isolates (See *Isolation of conjugative plasmids*) belonging to mating-pair formation type F, T and I and diverse incompatibility groups (Figure 2A). Of note, F-type plasmids harboured different TraN alleles (Figure 2A) which were recently shown to interact with surface receptors of recipient cells [71]. We set up an experimental design for plasmid conjugation including a short surface mating assay on lysogeny broth (LB) nutrient pads. The short period of time given to conjugation avoids the interference of potential differences in growth rates between donors and recipients, as well as having to account for transconjugants as donors [72,73]. We then computed the values of conjugation efficiency [72,73] (Figure S4ABC) (See *Conjugation assays*).

We performed a first set of assays (set E1) from a non-capsulated *E. coli* strain to the *K. pneumoniae* strains, including 10 plasmids, three recipient strains, and five capsule states (Δcps, K1, K2, K3, K24). The essays were done in triplicate, accounting for a total of 450 independent conjugation experiments. We used *E. coli* DH10B as a donor because it lacks defence systems, other plasmids, or even prophages, and is readily selectable. We observed measurable conjugation events for all pairwise strain-plasmid combinations, except for $p479_F$ in all three strains, and pP768-$NMD5_T$, $p486_T$ and $p580_{T/F}$ in strain ST45 (Figure 2A). When measurable, conjugation from an *E. coli* donor was significantly lower in capsulated strains than in the Δcps mutants in three out of four serotypes (Figure 2B, Wilcoxon tests, all $p<0.01$). This confirms and generalises our previous results using one single plasmid and Δ*wcaJ* mutants [12].

In a second set of experiments (set E2), we wished to understand the patterns of conjugation within the Kpn species, while controlling for the genetic background. We selected three plasmids – $p476_I$, $pKPN4_F$ and $pKP13d_T$ – which are from different MPF types and efficiently transferred from and to our three *K. pneumoniae* chassis strains (Figure 2A). We recovered the *K. pneumoniae* transconjugants of these plasmids and used them as donors to perform conjugation assays between all combinations of donors and recipients among the five capsule states (Δcps, K1, K2, K3, K24) in a total of 675 experiments. The capsulated strains of the four serotypes had significantly lower efficiencies of acquisition of plasmids by conjugation than the Δcps strains (Figure 2C, Wilcoxon test all $p<0.001$). Of note, the conjugation efficiencies of the pKPN4 plasmid alone were not significantly different between capsulated and non-capsulated cells (Paired Wilcoxon test, $p>0.05$). These results confirm that expression of a capsule is generally associated with lower rates of plasmid acquisition.

We then assessed if plasmid acquisition by conjugation is affected by the capsule serotype of the recipient cell. Considering all experiments (E1 and E2), pairwise comparisons between conjugation efficiencies across the combinations of serotypes showed that they were different for every pair of serotypes (Pairwise Wilcoxon tests, all $p<0.01$). We used this information to rank the serotypes from lower to higher median conjugation efficiencies, resulting in the following hierarchy: K1 < K2 < K24 < K3. We also observed that the impact of the recipient capsule serotype is dependent on the plasmid. This is especially evident for plasmid $pKPN4_F$ whose conjugation into capsulated strains was as efficient as into Δcps strains (grey points, Figure 2C, 2B). This was not due to higher intrinsic conjugation efficiency relative to the other plasmids, since $pKPN4_F$ displayed a median efficiency

between pKP13d$_T$ and p476$_I$ in E2 (Figure S4D). However, plasmid pKPN4$_F$ carried the TraNβ allele (Figure 2A), which recognizes *K. pneumoniae* OmpK36 L3 loop region [71]. We found that our three isolates encoded the *ompK36* gene with an intact L3 loop (See *TraN and TraN receptors typing*), leading to the hypothesis that TraN-receptor interactions may alleviate the impact of the capsule. Hence, the capsule negatively affects the acquisition of conjugative plasmids and its quantitative effect depends on the specific serotype and on the plasmid.

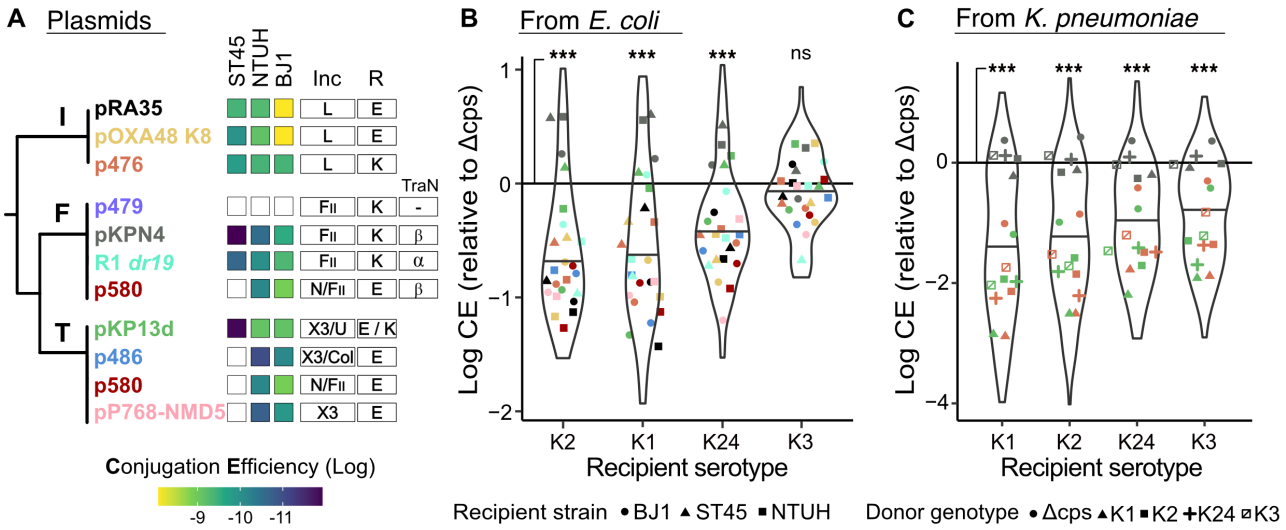

Figure 2 – Recipient's capsule and serotype influences conjugation efficiency. A. Conjugative plasmids included in the analysis. The plasmids are presented on a cladogram representing the evolutionary relations between the MPF types [38]. Note that p580 encodes two separate MPF systems of type F and T, but the F-type locus is interrupted by a transposon. Plasmid names colours match the colours of the points in the other panels. The three first columns correspond to the average conjugation efficiency (n=3) measured from *E. coli* to each of the three wild type strains. Additionally, we indicate the predicted incompatibility (Inc) groups, the antibiotic used for selection (R), either Ertapenem (E) or Kanamycin (K), and the TraN allele for F-type plasmids. **B.** Log_{10}-transformed conjugation efficiency (CE) relative to the associated Δcps mutant by capsule serotype of the recipient, from *E. coli* DH10B donors. Points represent the average of independent triplicates, with colours and shapes corresponding respectively to plasmids (panel A) and strains. Solid line at y=0 represents the conjugation efficiency of Δcps mutant. We used paired Wilcoxon tests to assess statistically significant differences. **C.** Same as panel B, but when conjugation takes place from *K. pneumoniae* donors. The shapes of the data points represent the genotype of the donor strain. Associated data are available as Supplementary Dataset S3 (Conjugation assays). *** $p<0.001$; ns $p>0.05$

Donor's serotype influences conjugation

There is no available information on the effect of capsules on the frequency of conjugation by the donor cell. To test the impact of the donor serotype on conjugation efficiency, we analysed our assays

relative to the capsule of the donor (including Δcps). This analysis was only done in the E2 set, since in E1 the donor is an *E. coli* strain lacking a capsule. The conjugation efficiency of Δcps cells was significantly higher than that of any of the four serotypes (Figure 3A). This difference was significant for plasmids pKP13d$_T$ and p476$_I$, but not for pKPN4$_F$. For the latter, the rates of conjugation seem independent of the presence of a capsule in the donor (just like above they seemed independent of the presence of a capsule in the recipient). In the case of the former (pKP13d$_T$ and p476$_I$), the efficiency of conjugation varied significantly between serotypes (Figure 3A). The rank of the serotypes in terms of efficiency of conjugation of the donor is similar to that identified above for the recipient: K1 < K2 < K24 < K3. Additionally, we tested if the impact the serotype was symmetrical between donors and recipients, *e.g.* if BJ1:K1→ NUTH:K2 is equivalent to BJ1:K2 → NTUH:K1. We found that conjugation efficiencies were not significantly different when comparing one direction to the other (Wilcoxon Paired test, p=0.8). Hence, conjugation efficiencies in donor and recipient cells are affected in similar ways by the presence and serotype of capsules.

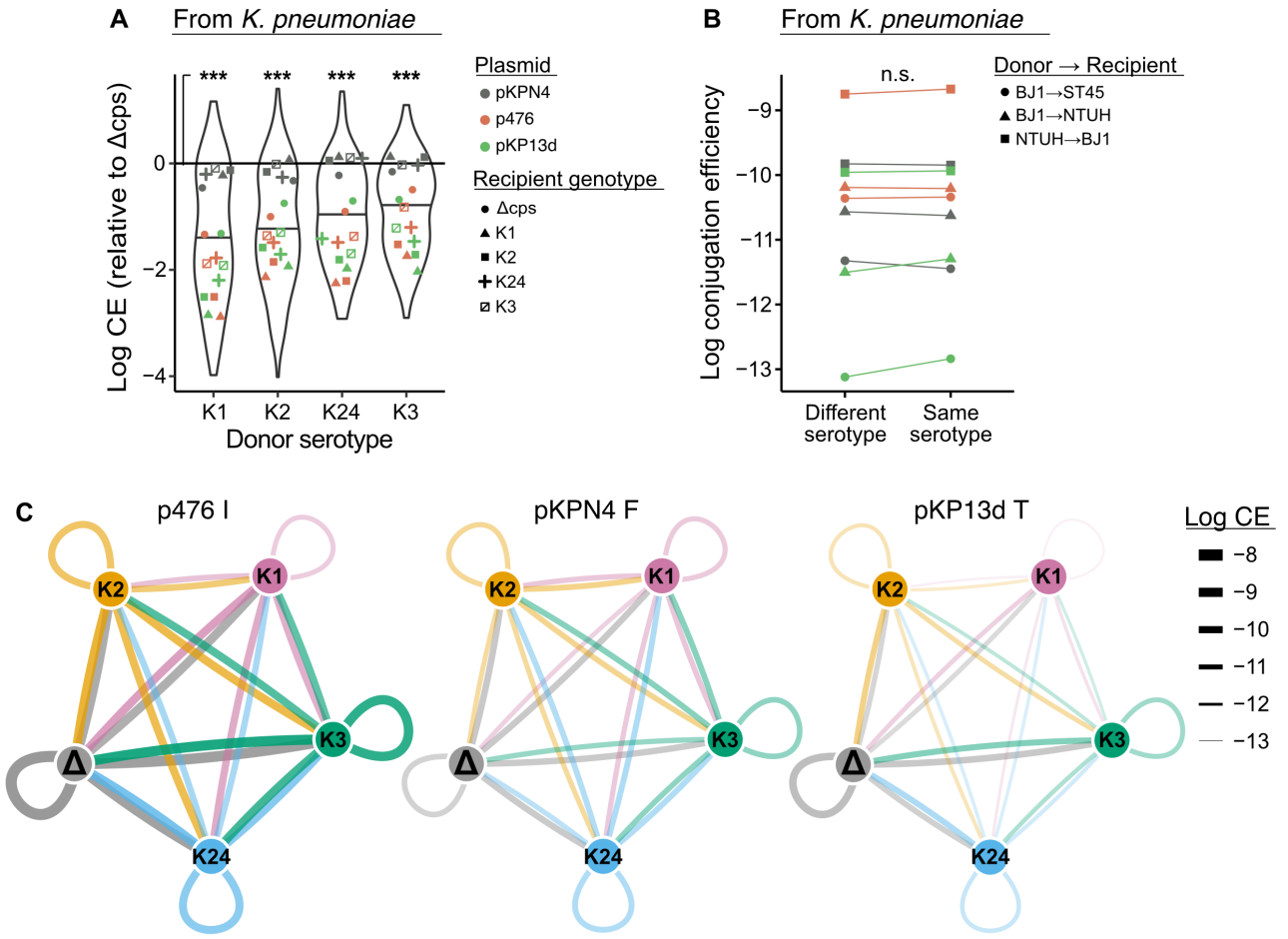

Figure 3 – Donor serotype influences conjugation efficiency. A. Log-transformed conjugation efficiency (CE) relative to the associated Δcps mutants by capsule serotype of the donor. Points represent the average of independent triplicates, with colours and shapes corresponding to strains and plasmids in Figure 2A. Solid line at y=0 represents the conjugation efficiency of Δcps mutant. All four serotypes are associated with significantly lower conjugation efficiencies than the Δcps mutants (Pairwise Wilcoxon, all p<0.001), but not when considering pKPN4 individually (all p>0.05). **B.** Log-transformed conjugation efficiency between pairs of donors and recipients with similar or

different serotypes. Points represent the mean conjugation efficiencies, colours correspond to the different plasmids (as in Figure 2 and 3) and shapes correspond to distinct pairs. Conjugation is not more efficient between donor and recipient expressing the same serotype, paired Wilcoxon test, P=0.9. **C.** Networks of plasmid transfer between capsule states. Data drawn from the *K. pneumoniae* to *K. pneumoniae* assays. Nodes represents distinct serotypes, and Δcps mutants. Edges thickness represents the average conjugation efficiency for all pairs. Edges are coloured according to the donor, indicating the direction of transfer. Associated data are available as Supplementary Dataset S3 (Conjugation assays).
*** $p<0.001$; ns $p>0.05$

Assessing the importance of the different variables on conjugation

The results above suggest that several variables affect the conjugation efficiency. Network analyses of conjugation efficiencies across serotypes confirm the relevance of the plasmid identity, of the serotype, and the similarity between the effects of donor and recipients (Figure 3BC). This results in wide differences in conjugation efficiency, i.e., in fast and slow lanes of horizontal gene transfer. This raises the question of the relative importance of each variable in plasmid transfer and how they jointly contribute to explain differences in conjugation efficiency.

We started by assessing if the MPF type is significantly associated with different conjugation efficiencies when accounting for the effect of the plasmid identity. For this, we used only the data of conjugation from *E. coli* (dataset E1) since in the other dataset (E2) we used three plasmids with a different MPF type each and one cannot distinguish between the two effects (MPF and plasmid identity). To test the hypothesis that MPF differ in conjugation efficiencies we used a linear mixed model where the MPF type was the fixed effect, and the plasmid identity was the random effect. This allows to test the effect of the MPF type while conditioning for the effect of the plasmid identity. We found that the effect of MPF is significant (Figure S4ABC, S5, F test, p =0.023). The comparisons of all pairs using a non-conditioned linear model shows that all pairs of MPF are significantly different and gives an order of efficiency of conjugation $MPF_F<MPF_T<MPF_I$ in both datasets E1 and E2 (Tukey-Kramer HSD test, p <0.001).

We then tested if the MPF type and serotypes affect the conjugation rates. We made a linear mixed model where we put together as fixed effects the MPF type of the plasmid and the serotypes of the donor and recipient, while conditioning (random effects) for the identity of the donor and recipient chassis strains. This analysis was done with dataset E2 (conjugation to and from *K. pneumoniae*), since in E1 there is no variation in the donor. The results showed that all three effects are significant (F tests, all p <0.001) (Figure S4DEF). Interestingly all parameter estimates of the fixed effects were also significant. Hence, differences within each group of variables, notably differences between serotypes both among donors and among recipients, were significant (t-tests, all p <0.05). We conclude that all three variables – MPF, donor, recipient serotypes - and that the categories within these variables all contribute significantly to explain the variation in conjugation efficiency.

Given that both donor and recipient serotypes are important for conjugation efficiencies, we tested the hypothesis that combinations of serotypes in donor and recipient cells could improve or decrease conjugation efficiency. For example, strains of the same serotype have been hypothesized to engage more efficiently in mating pair formation than pairs of strains with different serotypes [74]. To address this question, we used standard least squares to model the conjugation efficiency in function of the MPF type and the serotypes of donor and recipients. Here, we used only the data of conjugation between *K. pneumoniae* strains (dataset E2, since for dataset E1 the donor is never capsulated). We also added an interaction term between donor and recipient serotypes. This resulted in a significant linear model (R^2=0.43, p<0.001, F test), where the tests on the three variables revealed significant effect (p<0.001), but the interaction term was non-significant (p>0.9, same test). Accordingly, none of the comparisons between pairs of same vs. different capsule serotype were significantly different (Figure 3C). Thus, the capsule serotypes of the donor and recipient cells have a significant and independent impact on conjugation. Finally, one can have a coarse estimate of the relevance of the three significant variables by analysing individual ANOVA where each of the variables is fitted to the conjugation efficiency. While all tests were significant, the effect of the MPF type (R^2=0.32) was much larger than that of the donor serotype (R^2=0.07), which exceeded that of the recipient serotype (R^2=0.03). Hence, the MPF type might have a very important impact on conjugation efficiency, but such a conclusion will require further experiments with a much larger number of plasmids.

Capsule volume correlates negatively with conjugation efficiency

Having established the impact of capsule in conjugation, we set up to uncover a mechanism that could explain our observations: 1) higher conjugation efficiency is associated with the absence of capsule, 2) capsule serotypes affect the rate of conjugation, 3) there is no evidence of specific interactions between capsules of donors and recipients, i.e. conjugation efficiency is similar for pairs with similar or different capsules, (4) MPF pili, which are known to differ widely in length, are important determinants of conjugation efficiency. While (2) and (4) might suggest that some sort of receptor in the recipient cell could explain our results, (1) suggests that capsules are not being used as receptors for the pilus, and (3) suggests that specific interactions between the capsules of the donor and recipient cells are not important. We thus reasoned that the physical barrier represented by the capsule may impede cell-to-cell interactions, leading to inefficient mating-pair formation. To test the hypothesis that capsule volume explains differences in conjugation efficiencies, we measured the effective volume occupied by a cell in a colony (Figure 4A). On average for all three strains and capsule states, the average effective volume was 32 μm^3/CFU and a range of 10 to 75 μm^3/CFU. This is in line with previous estimates of the packing density of *E. coli* colonies grown in slightly different conditions (33 μm^3/CFU) [75]. As expected, non-capsulated cells have the smallest volume. This is not caused by a growth defect that could lead to small cells, since we have shown that in rich medium non-capsulated bacteria grow faster and should thus be larger once one excludes the effect of capsules [76]. As expected, all four serotypes were associated with significantly higher effective volumes than Δcps mutants. The K1 and K2 serotypes have the largest volume, which fits published data showing that natural strains with these serotypes tend to have very voluminous capsules [59,77]. Serotypes were associated with different effective volumes in the ranking order: K24/K3<K2<K1. For example, the effective volume of BJ1::K1 cells is on average *ca.* three times larger than that of BJ1::K3 cells.

These results confirm that a large fraction of the volume of the swapped strains can be explained by their different capsular types.

We then tested the hypothesis that capsule volume hinders conjugation by computing the association between the effective volume and conjugation efficiency. To do so, we fitted a linear mixed model with the cell volume as a fixed effect and the chassis strain as a random effect. The results show that the association between the capsule volume and conjugation efficiency is very strong once the identity of the chassis is considered (F test, $p<0.001$). To visualize the data in a simpler way, we made three linear regressions between the average effective volume and the average conjugation efficiency (all conjugation assays) for each chassis strain, which showed a good fit (Figure 4B). Hence, the effects of the chassis and of the capsule volume explain most of the variation in the conjugation efficiency between serotypes. The analysis of the slopes of these regressions shows that when the average effective cell volume decreases by 20 μm^3 there is roughly a doubling of the conjugation efficiency. These results are consistent with the hypothesis that capsule volume shapes conjugation efficiency.

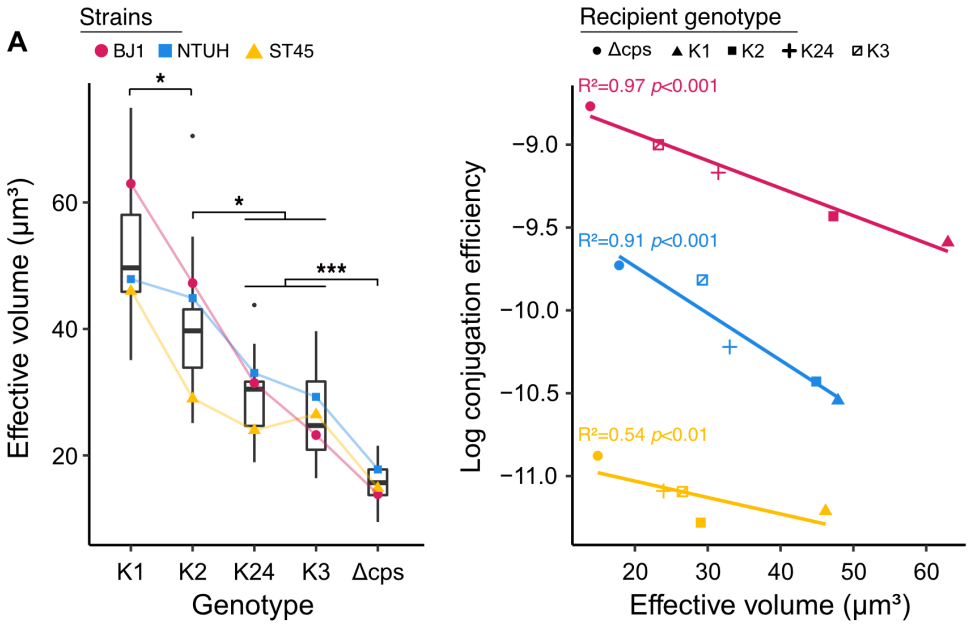

Figure 4 – Effective volume within colonies. A. Differences in effective volume (μm^3/CFU) between serotype swaps and Δcps mutants. We assessed statistical differences between volumes with an ANOVA followed by a Tukey's honestly significant difference test. The strain, genotype and their interaction significantly influenced the effective volume. All comparisons between genotypes were significantly different ($p<0.05$), except K24 and K3 ($p=0.85$), and genotypes were ranked according to the median effective volume. **B.** Average effective volume vs. average $\log_{10}$-transformed conjugation efficiencies (from E1 and E2). Points correspond to distinct capsule states in the recipient strain. Colour corresponds to the strains as in panel A. Lines represent linear regressions for each chassis strain between the $\log_{10}$-transformed conjugation efficiency and the average effective volume (EV). The linear mixed model of the $\log_{10}$ transformed conjugation efficiency using the effective volume as a fixed effect and the chassis strain identity as a random effect showed a significant effect of the volume (F test, p <0.001). Associated data are available as Supplementary Dataset S4 (Volume), Dataset S5 (Volume vs. recipient genotype) and Dataset S6 (Volume vs. donor genotype).

The determinants of conjugation shape the distribution of natural plasmids

Our analysis revealed that conjugation efficiency in the laboratory was strongly impacted by capsule expression and the serotypes of both donor and recipient cells, as well as by the MPF type. Do these results contribute to a better understanding of the distribution of plasmids in populations? We retrieved the non-redundant dataset of 623 complete genomes of *K. pneumoniae* from RefSeq, which contained 2,386 plasmids. We used these genomes to build a pangenome including 29,043 gene families. We extracted the pangenome gene families present in single copy in more than 90% of the strains and used these 3,940 gene families to build the species phylogenetic tree and used the genomic data to predict the capsule locus type of each strain (serotype). Finally, each plasmid was characterised in terms of the presence of the conjugation machinery, virulence factors, and antibiotic resistance genes. We found that 21% of the plasmids carried all the key genes for conjugation: 23% were of type MPF_I, 27% MPF_T, and 50% MPF_F. Some plasmids of all types carried antibiotic resistance genes (56% of all plasmids) but only Type F plasmids carried virulence factors (8%, half of which carried resistance genes too) (Figure 5A). Type F plasmids seem to be the least susceptible to the presence of a capsule and they also seem to be the most abundant across the species.

To assess if the rates of plasmid acquisition vary with the serotype, we traced the history of acquisition of each plasmid on the species tree. We found that 68% of the conjugative plasmids were acquired in terminal branches, implying that conjugative plasmids in this dataset were acquired very recently. We then searched to understand if there is an association between the relative frequency of conjugation of each serotype (as measured in the laboratory) and the frequency of acquisition of plasmids by strains in populations of these serotypes. More precisely, we tested if the number of conjugative plasmids acquired on the terminal branches of the tree differed between groups of serotypes. We focused on acquisitions in terminal branches because these are more accurately inferred, and this procedure allows to only count independent events. We observed that serotypes differ in the rate of acquisition of conjugative plasmids (Kruskal-Wallis test, $p<0.001$). We then focused on the serotypes included in this study, namely K1, K2, K3, and K24 (Figure 5B). We computed for each serotype the median number of recent plasmid gains. While there were only seven genomes encoding a K3 capsule locus type, rendering the statistical power of the analysis weak, we observed that the ranking of these values matches the ranking of the conjugation efficiency, *i.e.* the serotypes gaining more plasmids in the terminal branches of the tree (K3 and then K24) are those for which we found lower capsule volumes (Figure 4A) and higher conjugation efficiencies (Figure 2A, 2B, 3A). These results suggest that the impact of the capsule serotype on conjugation efficiency translates in different rates of plasmid acquisition in natural populations.

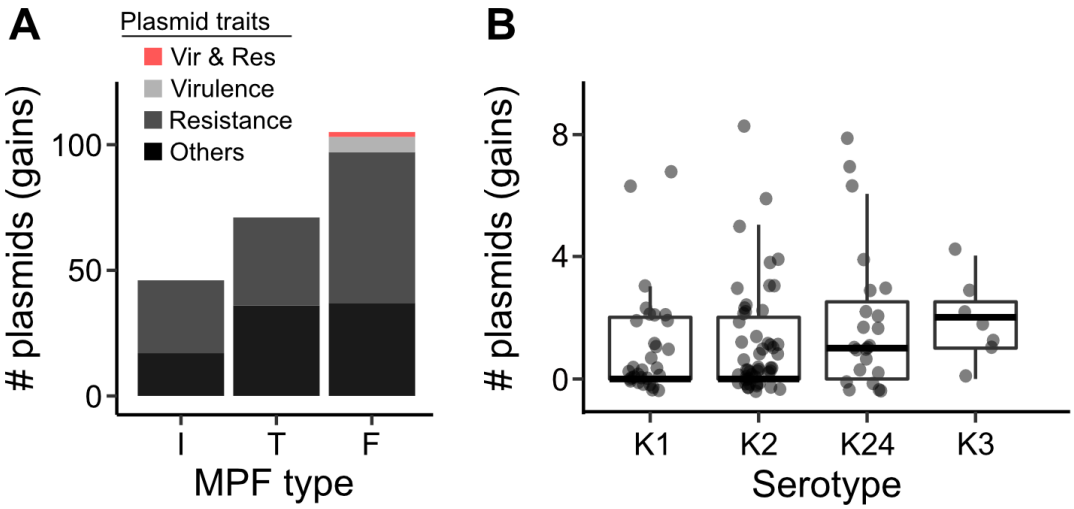

Figure 5 –Distribution of recently acquired conjugative plasmids. Analysis of 623 complete *K. pneumoniae* genomes. **A.** Number of conjugative plasmids acquired recently in the genomes of our dataset (Supplementary Dataset S7). The colours correspond to the different categories of plasmids. The data correspond to conjugative plasmids acquired in terminal branches. **B.** Number of plasmids recently acquired (terminal branches of the species tree) in different serotypes (Supplementary Dataset S8).

Discussion

Bacteria have multiple mechanisms to restrict infections by MGEs, including intracellular defense systems [78] and surface exclusion systems [79]. They also encode an array of functions with pleiotropic effects on these infections, e.g. involved in DNA repair [80] or present at the cell envelope [81]. Among the latter, the capsule protects from abiotic stresses and the host immune system, but is also regarded as a gatekeeper for phages and plasmids. Here we precisely quantified these latter effects in *K. pneumoniae* using isogenic serotype-swap mutants in three different chassis strains. Remarkably, the acquisition of a capsule locus of *c.a.* 25kb in place of the original and its expression did not require additional mutations. This suggest that capsules loci might be transferred easily within the *K. pneumoniae* population where they are ready-to-express, as previously observed in bacteria with high transformation efficiencies such as *Streptococcus pneumoniae* [82]. Such mutants will be useful in the future to probe interactions between capsules, MGEs and other cellular components, e.g. to understand how genetic backgrounds may shape the serotype swaps that hamper capsule-based vaccines long-term efficacy [83,84].

Phage infection requires the availability of a specific receptor at the cell surface. This affects bacterial population dynamics and our ability to leverage phages for antimicrobial therapy. Capsules can mask receptors present on the cell surface, and thus act as barriers to phage infection [85–87]. They can also be necessary for phage infection, especially in nearly ubiquitously capsulated species like *Serratia* [88], *Acinetobacter* [89] or *Klebsiella* [24]. The host range of capsule targeting phages is generally restricted to one or a few serotypes [24,90], because they rely on the tail spike proteins harbouring depolymerase enzymes [91,92] that act as specific receptor-binding proteins tunnelling through capsules [93]. Here, we found that sensitive strains to capsule-dependent phages all became resistant upon capsule inactivation or serotype swap. We also showed that the acquisition of a new serotype resulted in the inversion of phage sensitivity, as swapped strains became sensitive to phages that could infect the original donor of the capsule. Hence, these results show that independently of the genetic background, the loss or swap of capsules is often necessary and sufficient to change the sensitivity of *K. pneumoniae* to phages.

We examined the influence of the capsule (and its serotype) on conjugation, building on previous findings that showed that the capsule can decrease the rate of acquisition of one specific conjugative plasmid [12]. Our results on a diverse panel of plasmids, donor, and recipient strains show that the presence of capsules in both the donor and recipient cells usually reduces the efficiency of conjugation. Of note, a recent study on the conjugation of pOXA48 suggests that the effect of capsules may even be stronger in other species, since those of *Klebsiella* were the ones less hindering transfer [94]. Importantly, the number of recent plasmid acquisitions in natural populations matches the *in vitro* estimated rates of conjugation, *i.e.*, serotypes more permissive to conjugation in the lab correspond to those having acquired more plasmids recently in natural populations. Furthermore, this effect depends on the serotype. Capsules of the K1 and K2 serotypes, which are the most frequent among hypervirulent isolates resistant to phagocyte-mediated clearance [6,95,96], are particularly effective at blocking conjugation. The capsules of these hypervirulent isolates are often very thick which may facilitate escape to the immune system [59], but also hamper conjugation. Nevertheless, we observed some heterogeneity in the susceptibility to the capsule among the plasmids. For example,

pKPN4$_F$ seems to transfer independently of the capsule. This may be due to the presence of the TraNβ allele in the MPF$_F$ apparatus, which was recently shown to stabilize mating-pair formation with *K. pneumoniae* recipients [71,95,97,98] and is present in the MPF system of pKNP4$_F$. Understanding how different factors like TraNβ and the capsule affect conjugation may represent a fruitful venue for future research. Since MPF$_F$ plasmids spread more efficiently in the heavily capsulated cells of hypervirulent strains, this would explain why we found virulence factors exclusively on this type of conjugative plasmids. If so, our results suggest the existence of a trade-off between virulence (the ability to evade the immune system) and evolvability (the ability to exchange genetic material with other bacteria). This trade-off seems partly alleviated in MPF$_F$ plasmids, which may have contributed for their huge success in this species and to their unique carriage of both virulence factors and recently acquired antibiotic resistance genes. The reunion of the two traits in such conjugative plasmids has led to the recent emergence of hyper-virulent and resistant clones [99]. We propose that the ability to conjugate independently of the capsule may be a hallmark of conjugative plasmids conferring hyper-virulence and multi-drug resistance.

The effect of capsules on conjugation is intriguing and could arise in multiple ways. We show that it does not depend on interactions between serotypes, suggesting that the effect of capsules is not specifically linked with their composition. Instead, the volume taken by the capsule seems to explain a lot of the variation in conjugation rates between otherwise isogenic strains. The capsulated cells occupy more volume than non-capsulated cells in bacterial colonies, and capsule serotypes are associated with different cell effective volumes. For example, K1-expressing cells occupy up to three times more space than non-capsulated cells and conjugate at much lower rates. Moreover, capsule-mediated increase in effective volume is strongly associated with decrease in conjugation efficiency, *i.e.* the more space a cell takes up, the less efficient it is at conjugation. This suggests that the capsule may affect conjugation by physically distancing the bacteria from each other, making it harder for plasmids to be transferred between them by conjugation. This model can also explain the different interactions between capsules and MPF types, since Type T and I are typically short, non-retractile, and are very much affected by the distance imposed by the capsule. In contrast, the F-pili are longer and can retract, which may allow them to bypass spatial hindrance and could explain why they seem much less affected by the presence of capsules.

Transduction, lysogeny and conjugation mediate HGT in most bacterial species. Consequently, factors that influence the rates of infection by phages and conjugative elements shape gene flow [35,65]. In this study, we examined the capsule's dual role in determining phage susceptibility and modulating conjugation efficiency. Our results demonstrate that cell envelope structures play a crucial role in bacterial species evolution. Since capsules are frequently exchanged in natural populations, clones can undergo drastic changes in their ability to access new gene pools following serotype swaps. Changing the capsule type can close or open new routes for phage-mediated HGT and slow down or accelerate plasmid transfer rates. These observations are consistent with previous findings that the transfer of prophages, but not that of conjugation systems, is biased toward same-serotype exchanges [12].

Our results on the role of capsules on conjugation and phage infection can be of relevance to understand other mechanisms affecting capsulated cells and shaping their ecological interactions

[100], notably those concerning mechanisms that deliver effectors into other cells. For example, T4SS are part of the MPF leading to plasmid conjugation, but are also used by pathogens to inject proteins and toxins in eukaryotic [37,100,101] and bacterial cells [102]. We suspect that capsules may hinder the attackers and protect the victims from T4SS. Capsules may also offer protection from other syringe-like devices like the type III [103] and type VI [104,105] secretion systems. Accordingly, capsules protect enterobacterial cells, including *K. pneumoniae*, from T6SS killing [106,107]. Extracellular contractile injection systems (eCIS) are toxin-delivery particles that evolved from phages [108]. Capsules might be a protective barrier from eCIS. When the latter specifically target the capsule, like many phages do, then serotype variation may allow bacteria to escape [109]. Capsules may thus impact virulence, population dynamics, bacterial competition and horizontal gene transfer in multiple ways.

Materials and methods

Strains and plasmids

The strains used in this study, as well as their genomic annotations and accession numbers, are described in Table S1. The conjugative plasmids used in this study are described in Table S2.

Scarless serotype swaps

The detailed protocol for scarless serotype swaps is available as Supplementary Text 1. Briefly, we first constructed complete capsule loci deletion (Δcps mutants) in our target strains via a Lambda Red knockout with a modified KmFRT cassette including an I-SceI cut site outside the Flp recognition target (FRT) sites, and 500 bp of homology upstream *galF* and downstream *ugd*. The KanMX marker was then excised via expression of the FLP recombinase, leaving an 80bp scar containing the I-SceI cut site between *galF* and *ugd*, which were left intact (Supplementary Table S3, *primers*).
We cloned the whole capsule loci (~30kb) from strains with distinct capsule serotypes via a Lambda Red gap-repair cloning approach. We cloned capsular loci from the strains involved in the swaps for K2 (BJ1) and K24 (ST45). Capsule locus K1 was cloned from *K. pneumoniae* SA12 (ERZ3205754) which harbour a nearly identical locus as NTUH-K2044 (>99% identity, >99% coverage). Capsule locus K3 was cloned from the reference strain *K. pneumoniae* ATCC 13883.
We built a cloning cassette encoding a KanMX resistance marker, an I-SceI cut site, and low copy pSC101 origin of replication. This cassette is designed to circularize around the capsule locus, including *galF* promoter and *ugd* stop codon, via recombination to capture the whole locus onto a vector, hereafter referred to as pKapture (Supplementary Table S3, *primers*).
We electroporated pKapture vectors in the Δcps mutants, effectively complementing capsule expression *in trans* with their own, or other, capsule loci. To force integration of the cloned capsule into its native site, the Δcps strains transformed with pKapture were electroporated with the pTKRED plasmid [110], carrying an inducible I-SceI restriction enzyme, inducible Lambda Red system, and a functional copy of *recA*. Briefly, we induced the I-SceI enzyme overnight with selection to maintain pTKRED. The I-SceI enzyme linearizes the pKapture plasmid, providing recombination proficient linear ends, and introduce a chromosomal double-strand break within the capsule deletion, which is lethal if unrepaired, resulting in the insertion of the capsule locus. When the repair occurs with the linearized plasmid, the I-SceI cut site is removed since the capsule locus recombines outside of the deletion. We identified capsulated colonies on LB plates without selection, and sequenced the mutants to validate the proper scarless replacement of the capsule locus. We performed whole-genome sequencing of the swaps by Illumina and used Breseq v0.36 [111] to verify off-target mutations (see *Mutants and transconjugants validation*). All the 12 strains we sequenced carried the expected capsule swap and only one strain carried one missense mutation in the gene *pheP* (NTHUH::K24), located outside the capsule locus.

Phage assays

i)Phage details. Phage lysates of phK1, phK2 and phK24 were obtained from various laboratories and streaked for single plaques on lawns of the wildtype strains NTUH (phK1), BJ1 (phK2), and ST45 (phK24). Phage phK1 was described in [112]. Phages phK2 and phK24 were isolated from sewage from wastewater treatment plants in Valencia (Spain). The former was isolated using *K. pneumoniae* B 5055 capsular type KL2 as host, and phK24 was using *K. pneumoniae* 1680/49 capsular type KL24. Both strains were purchased from the Statens Serum Institute (Copenhagen). For phage isolation, sewage samples were filtered and tested on soft agar semi-solidified media containing a lawn of the *K. pneumoniae* strains.
To isolate each phage, a triple plaque-to-plaque transfer was carried out. Subsequently, each isolated plaque was used to infect log-phase *K. pneumoniae* cultures, and the supernatants were titrated by the standard plaque assay.

ii) *Phage production.* After overnight incubation, three independent plaques were picked for each phage with a sterile tip and co-inoculated with a single colony of the host strain in 5mL of fresh LB at 37°C. The co-culture was spun down the next day and the supernatant was filtered through 0.22um. 10uL of each filtrate was introduced in exponentially growing cultures (OD = 0.4) of its corresponding host. Complete lysis was evident for all three phages after 3h. To recover phage particles, the cultures were centrifuged at 4000 rpm. Supernatants were mixed with chilled PEG-NaCl 5X (PEG 8000 20% and 2.5M of NaCl) through inversion. Phages were allowed to precipitate for 15 min and pelleted by centrifugation 10 min at 13000 rpm at 4°C. The pellets were dissolved in TBS (Tris Buffer Saline, 50 mM Tris-HCl, pH 7.5, 150 mM NaCl).
iii)*Phage infections.* To test the susceptibility of wildtype, Δcps mutants, and capsule swapped strains to phages, overnight cultures in LB of strains were diluted 1:100 and allowed to grow until OD = 0.8. 250 µL of bacterial cultures were mixed with 3 mL of top agar (0.7% agar) and poured intro prewarmed LB plates to generate the bacteria overlay. Plates were allowed to dry before spotting serial dilutions of PEG-precipitated phages. Plates were incubated at 37°C for 4 hours and plaques were counted. The lysate titer is defined as the concentration obtained by estimating the plaque forming unit per ml on the lawn of the strain used to prepare the phage lysate.
iv) *Phage adsorption*. To test the ability of a phage to adsorb, we mixed 10uL of phage stock solution with 500uL of overnight bacterial culture for 5min 37°C. We then placed the tubes in ice, and transferred them in a pre-chilled centrifuge at 4°C. After centrifugation for 5min 13000 rpm, we spotted serial dilution of the supernatant on bacterial lawns of the phage host for PFU counting.

Selection and characterization of conjugative plasmids

i)*Plasmid identification.* We screened the genomes of our laboratory collection and the isolates of the National Reference Center (Centre National de Reference) for Carbapenemase-producing Enterobacteriaceae at the Bicêtre Hospital (Paris) to identify contigs resembling conjugative plasmids. We used Plasmidfinder [113] to retrieve plasmid contigs, MacSyFinder with TXSScan models [67,114] to identify conjugation operons and annotate their mating-pair formation type, and ResFinder to annotate antibiotics resistance genes [115]. We gathered a list of contigs containing the following features: a plasmid replicase identified and typed by PlasmidFinder, a complete conjugation system, and at least one selectable antibiotic resistance (carbapenem or kanamycin resistance, absent in our swapped strains). Additionally, we included two extensively studied

conjugative plasmids, pOXA48-K8 (MPF_I) and the de-repressed version of the R1 plasmid, R1 *dr19* (MPF_F) [116]. We purified our plasmids of interest by conjugation into *E. coli* DH10B, which does not encode any prophage, plasmid, restriction-modification system, and is resistant to streptomycin and auxotroph for leucine. We picked one transconjugant per plasmid, and sequenced it to validate that they only contained a single conjugative system (see *Mutants and transconjugants validation*). Those plasmids are described in Table S2.

ii)*Plasmid annotation.* To detect conjugative systems and infer their MPF types, we used TXSScan with default options [37,117]. To detect and annotate virulence factors, we used Kleborate v2.2 [118] with default options. To detect and annotate antibiotics resistance genes, we used ResFinder v4.0 [115]. We classed plasmids into distinct categories, "resistance plasmids" containing at least one ARG, "virulence plasmids" containing at least one virulence gene, "virulence and resistance plasmids" containing at least one virulence and one resistance gene, and the rest of the plasmids as "others".

iii) *TraN and TraN receptors typing.* We gathered the sequences of TraN proteins described in [71] (Supplementary File S4) and searched for homologs among the MPF-F plasmids proteins with Blastp v2.10.0+ [119]. The best hits based on the bitscore of the alignment are displayed in Table S5. OmpK36 proteins were identified as the best hit (bitscore) of a Blastp search (Table S5) with WP_004180702 (NCBI accession) and aligned with Clustal Omega (Figure S6). The L3 and L4 regions are highlighted according to [71]. OmpA homologs were found through a Blastp search (Table S5) with NP_415477 (NCBI accession), and the best hit (bitscore). All three OmpA are 100% identical.

Mutants and transconjugants validation

We performed DNA extraction with the guanidium thiocyanate method [120], with modifications. DNA was extracted from pelleted cells grown overnight in LB supplemented with 0.7 mM EDTA and appropriate antibiotics for plasmid maintenance. Additionally, RNAse A treatment (37°C, 30 minutes) was performed before DNA precipitation. Each clone was sequenced by Illumina with 150pb paired-end reads from NextSeq 550, yielding approximately 1 GB of data per clone. The raw data were deposited in the BioProject PRJNA952961.

All mutants generated in this study were verified by whole-genome sequencing and comparison to the reference wildtype genome with Breseq v0.37.0 with default options [111] (Supplementary File S6). We also assembled the genomes *de novo* with Spades v3.15.5 [121] (option *-isolate*) and ran Kaptive [122] to annotate and extract the inserted capsule locus. Annotations corresponded with the expected insertion, and alignment of the extracted capsule locus to the source strain with EMBOSS Needle [123] revealed no mutation.

All DH10B transconjugants used as donors were also verified by whole-genome sequencing (Illumina paired-end 300bp reads), to verify that only the target plasmid and no other MGEs were transferred. To do so, we assembled the genomes with Spades v3.15.5 [121] (option *-isolate*) and analysed the assembly to find plasmid contig(s) as described above in *Isolation of conjugative plasmids*. We found only one plasmid contig per assembly. We used Blastn v2.10.0+ [119] to check that the plasmid

contig in DH10B matched one contig from the original donor strain, which was the case. Finally, we extracted and circularized the plasmid contig in DH10B with SnapGene (Supplementary File S3), according to i) the paired-end read mapped with bwa-mem v0.7.17 [124] and visualized in IGV [125] ii) the assembly of the plasmid contig in the original donor strain and iii) long-reads obtained via low-coverage (10x) Pacbio sequencing of the original donor strain that were mapped onto the assembly with bwa-mem v0.7.17 (BioProject: PRJNA952961).

Conjugation assays

i)Experimental setup. E. coli donors were cultured overnight from a single colony with the appropriate antibiotic in 3mL LB at 37°C. The next day, cultures were prepared from a 1:50 dilution. *K. pneumoniae* donors and recipients were inoculated over day from single colonies into 3mL fresh LB with the appropriate antibiotics to avoid the emergence of non-capsulated cells that can appear rapidly under laboratory conditions [126]. We used ertapenem with a final concentration of 0.15 µg/ml for plasmids encoding a carbapenemase and kanamycin with a final concentration of 50 µg/ml for plasmids encoding aminoglycoside resistance genes (see Table S2).
Cells reached an OD600 ≈ 1 after 4h of over-day growth, point at which donor cultures were centrifuged and resuspended in 3mL phosphate-buffered saline (PBS). They were then mixed 1:1 (vol:vol) and a 15µL drop of the mixture was inoculated on a 24-well microtiter plate containing 1mL LB agar pads. The droplets were allowed to dry under the hood with laminar flow (5-10min) and incubated for 1h in a humidity box at 37°C. Then, 1mL PBS was added in each well, and the plates were sealed with a hydrophobic adhesive film and shaken at 120rpm for 5min to resuspend the lawn. The contents of each well were then transferred to a 96-well plate, serially diluted and spotted (10µL) on plates selecting for either donor cells, recipient cells, or transconjugants. The next day, colonies were counted at the appropriate dilution (between 3 and 30 colonies per spot).
ii) *Selective plating.* We used a selective plating strategy to enumerate exclusively the donors, recipients and transconjugants. To do this, we leveraged the natural markers of our focal strains. This strategy is recapitulated in table S5.
iii) *Conjugation efficiency estimation***.** To measure the transfer of conjugative plasmids, we computed the transfer rate constant [127], or conjugation efficiency [128], with the following method:

$$\text{Conjugation efficiency } = \frac{T}{DR} \cdot \Delta t$$

Where T is the transconjugants concentration (CFU/mL), D the donors concentration, R the recipients concentration and Δt is the time of conjugation. This quantity is expressed in $mL.CFU^{-1}.hours^{-1}$ and represents the transfer rate constant [72]. This method performs accurately to estimate the efficiency of conjugation, especially under short conjugation time which minimize the impact of transconjugant conjugation. It was shown to produce consistent estimates of the D:R ratio when compared with far more complex population-based methods [72,73].
We also compared this quantity with the widely used, and simpler formula T/R, and found a Pearson correlation coefficient of 0.97 (p<0.001) between the two quantities after log-transformation. Hence, these two values are highly correlated and may be interchangeable under our conditions. All analyses

were performed with the conjugation efficiency formula above, since it was shown to be less susceptible to experimental parameters [72,73]. The data are available in Supplementary Dataset S3.

Effective volume measurement

We inoculated a 15 µL drop from an overnight culture for each strain onto LB agar plates and incubated the plates at 37°C. After 24h of growth, we resuspended each colony into 1.5mL Eppendorf tubes containing 50µL of PBS. Tubes were vortexed for 1min, then left for 15min at room temperature, and vortexed again for 1min. This allowed for complete dissolution of colonies. We then used a 0.5-10µL micropipette to measure the excess volume. In parallel, we performed serial dilutions followed by plating on LB agar to estimate the total number of CFU in the resuspended colony. The effective volume was then computed as the ratio of CFU by the volume of the colony. This quantity represents the average volume occupied by a cell in a colony. The data are available in Supplementary Dataset S4, S5 and S6.

Genome data

We retrieved all the *K. pneumoniae* complete genomes available in the NCBI non-redundant RefSeq database, accessed in March 2021, along with their gene annotations. This resulted in a set of 730 genomes containing 2386 associated plasmids. The pairwise genetic distances between all genomes of the species was calculated using MASH [129]. Strains that were too divergent (MASH distance >6%) to the reference strain or too similar (<0.0001) to any other strains were removed from further analysis. A total of 623 genomes were analysed. The information on the genomes (including accession numbers) is available in Supplementary Dataset S7.

Pan and persistent genomes

The pangenome is the full repertoire of homologous gene families in a species. The pangenome of *K. pneumoniae* was identified using the module pangenome of the software PanACoTa [130] v1.3.1. Briefly, gene families were built with MMseqs2 v13.45111, with an identity and bi-directional coverage threshold of 80%. This analysis resulted in 29,043 gene families among the 623 genomes (Supplementary Dataset S8). We then computed the persistent genome with a persistence threshold of 90%, meaning that a gene family must be present in single copy in at least 90% of the genomes to be considered persistent, and found 3,940 gene families.

Phylogenetic inference

To compute the species phylogenetic tree, we aligned each of the 3,940 protein families of the persistent genome individually with the align module of PanACoTA. These alignments were concatenated to produce a large alignment matrix with 296,147 parsimony-informative sites over a total alignment of 3,740,313 bp. We then use this alignment to make the phylogenetic inference using IQ-TREE (v2.02). We used ModelFinder [131] and calculated 1,000 ultra-fast bootstrap [132]. The

best-fit model was a general time-reversible model with empirical base frequencies allowing for invariable sites and discrete Gamma model with 4 rate categories (GTR+F+I+G4). We rooted the phylogenetic tree with the *midpoint.root()* function from the Phangorn R package [133]. The tree is available as Supplementary File S5.

Capsule locus typing

We used Kaptive [122,134] with default options and the "K locus primary reference" to identify the capsule locus type (CLT) of strains. The predicted CLT is assigned a confidence level, which relies on the overall alignment to the reference CLT, the allelic composition of the locus, and its fragmentation level. We assigned the CLT to "unknown" when the confidence level of Kaptive was indicated as "none" or "low," as suggested by the authors of the software. The annotation is available in Supplementary Dataset S9.

Reconstruction of the scenario of plasmid gain.

We used inference of ancestral states to identify the branches in the tree where the plasmid was acquired. For this, we inferred the ancestral state of each plasmid pangenome family with PastML (v1.9.23) [135] using the MAP algorithm and the F81 model. For each of these gene families, we obtained a list of branches where they were acquired. Genes from the same plasmid can come out of this analysis has having been acquired at different branches if there were changes in the plasmids after acquisition (gene gains or gene losses). To identify the plasmids most likely acquired in the terminal branches of the of the species tree, we counted how many genes of the plasmid were acquired in these branches. We defined that a plasmid was acquired in the terminal branch if at least 75% of its genes were inferred to be absent in the first parental node (*i.e.* acquired since then). Those are referred as recent gains. The other plasmids were not considered in the analysis presented on Figure 5. The data are available in Supplementary Dataset S10.

Data analysis and availability

All the data analyses were performed with R version 4.2 and Rstudio v2022.02.1, except linear mixed models which were computed in JMP v16 (SAS corporation). The statistical tests were performed with the base package *stats*, except type II ANOVA which were performed with the function Anova() from the *car* package v3.1 [136]. For data frame manipulations, we also used *dplyr* v1.0.10 along with the *tidyverse* packages [137] and *data.table* v1.12.8. We used the packages *ape* v5.3 [138], *phangorn* v2.5.5 [133], and *treeio* v1.10 [139] for the phylogenetic analyses.

Acknowledgements

We thank Olivier Tenaillon and Nienke Buddelmeijer for fruitful discussions. We thank Sylvain Brisse for providing us with the *Klebsiella* strains. We thank Jean-Marc Ghigo and Christophe Beloin for the gift of plasmid R1-*dr19*. We thank Julia Bos for the gift of phage phK1. We are grateful to Maxime Policarpo, Grégoire Haouy, Léone Debarge and the members of the Microbial Evolutionary

Genomics lab for helpful discussions. This work used the computational and storage services (TARS & MAESTRO cluster) provided by the IT department at Institut Pasteur, Paris, and the media preparation services proved by the Plateforme Milieux. The sequencing work was performed by the Biomics Platform, C2RT, Institut Pasteur, Paris, France, supported by France Génomique (ANR-10-INBS-09) and IBISA.

Funding

This work was supported by an ANR JCJC (Agence national de recherche) grant [ANR 18 CE12 0001 01 ENCAPSULATION] awarded to O. R. and by the grant [ANR 16 CE15 0022 03 PREDIRES] awarded to EPCR. The laboratory is funded by a Laboratoire d'Excellence 'Integrative Biology of Emerging Infectious Diseases' grant [ANR-10-LABX-62- IBEID], the INCEPTION program[PIA/ANR-16- CONV-0005], and the FRM [EQU201903007835]. M.H. has received funding from the FIRE Doctoral School (Centre de Recherche Interdisciplinaire, programme Bettencourt) to attend conferences. P.D.-C. was financially supported by a Ramón y Cajal contract RYC2019-028015-I funded by MCIN/AEI/10.13039/501100011033, ESF Invest in your future. The funders had no role in the study design, data collection and interpretation, or the decision to submit the work for publication.

References

1. Tipton KA, Chin C-Y, Farokhyfar M, Weiss DS, Rather PN. Role of Capsule in Resistance to Disinfectants, Host Antimicrobials, and Desiccation in Acinetobacter baumannii. Antimicrob Agents Chemother. 2018;62. doi:10.1128/AAC.01188-18
2. Scholl D, Adhya S, Merril C. Escherichia coli K1's capsule is a barrier to bacteriophage T7. Appl Environ Microbiol. 2005;71: 4872–4874. doi:10.1128/AEM.71.8.4872-4874.2005
3. Soundararajan M, von Bünau R, Oelschlaeger TA. K5 Capsule and Lipopolysaccharide Are Important in Resistance to T4 Phage Attack in Probiotic E. coli Strain Nissle 1917. Front Microbiol. 2019;10: 2783. doi:10.3389/fmicb.2019.02783
4. Jung S-Y, Matin A, Kim KS, Khan NA. The capsule plays an important role in Escherichia coli K1 interactions with Acanthamoeba. Int J Parasitol. 2007;37: 417–423. doi:10.1016/j.ijpara.2006.10.012
5. Hyams C, Camberlein E, Cohen JM, Bax K, Brown JS. The Streptococcus pneumoniae Capsule Inhibits Complement Activity and Neutrophil Phagocytosis by Multiple Mechanisms. Infect Immun. 2010;78: 704–715. doi:10.1128/IAI.00881-09
6. Kostina E, Ofek I, Crouch E, Friedman R, Sirota L, Klinger G, et al. Noncapsulated Klebsiella pneumoniae bearing mannose-containing O antigens is rapidly eradicated from mouse lung and triggers cytokine production by macrophages following opsonization with surfactant protein D. Infect Immun. 2005;73: 8282–8290. doi:10.1128/IAI.73.12.8282-8290.2005
7. Rice LB. Federal funding for the study of antimicrobial resistance in nosocomial pathogens: no ESKAPE. J Infect Dis. 2008;197: 1079–1081. doi:10.1086/533452
8. Rendueles O, Garcia-Garcerà M, Néron B, Touchon M, Rocha EPC. Abundance and co-occurrence of extracellular capsules increase environmental breadth: Implications for the emergence of pathogens. PLOS Pathog. 2017;13: e1006525. doi:10.1371/journal.ppat.1006525
9. Whitfield C, Wear SS, Sande C. Assembly of Bacterial Capsular Polysaccharides and Exopolysaccharides. Annu Rev Microbiol. 2020;74: 521–543. doi:10.1146/annurev-micro-011420-075607
10. Whitfield C. Biosynthesis and assembly of capsular polysaccharides in Escherichia coli. Annu Rev Biochem. 2006;75: 39–68. doi:10.1146/annurev.biochem.75.103004.142545
11. Mostowy RJ, Holt KE. Diversity-Generating Machines: Genetics of Bacterial Sugar-Coating. Trends Microbiol. 2018;26: 1008–1021. doi:10.1016/j.tim.2018.06.006
12. Haudiquet M, Buffet A, Rendueles O, Rocha EPC. Interplay between the cell envelope and mobile genetic elements shapes gene flow in populations of the nosocomial pathogen Klebsiella pneumoniae. PLoS Biol. 2021;19: e3001276. doi:10.1371/journal.pbio.3001276
13. Croucher NJ, Kagedan L, Thompson CM, Parkhill J, Bentley SD, Finkelstein JA, et al. Selective and Genetic Constraints on Pneumococcal Serotype Switching. PLoS Genet. 2015;11. doi:10.1371/journal.pgen.1005095
14. Weitz JS, Poisot T, Meyer JR, Flores CO, Valverde S, Sullivan MB, et al. Phage-bacteria infection networks. Trends Microbiol. 2013;21: 82–91. doi:10.1016/j.tim.2012.11.003
15. Rendueles O, Sousa JAM de, Rocha EPC. Competition between phage-resistance mechanisms determines the outcome of bacterial co-existence. bioRxiv; 2022. p. 2022.07.11.499539. doi:10.1101/2022.07.11.499539
16. Rousset F, Cui L, Siouve E, Becavin C, Depardieu F, Bikard D. Genome-wide CRISPR-dCas9 screens in E. coli identify essential genes and phage host factors. PLOS Genet. 2018;14: e1007749. doi:10.1371/journal.pgen.1007749
17. Rieger-Hug D, Stirm S. Comparative study of host capsule depolymerases associated with Klebsiella bacteriophages. Virology. 1981;113: 363–378. doi:10.1016/0042-6822(81)90162-8

18. Bertozzi Silva J, Storms Z, Sauvageau D. Host receptors for bacteriophage adsorption. FEMS Microbiol Lett. 2016;363: fnw002. doi:10.1093/femsle/fnw002
19. Pires DP, Oliveira H, Melo LDR, Sillankorva S, Azeredo J. Bacteriophage-encoded depolymerases: their diversity and biotechnological applications. Appl Microbiol Biotechnol. 2016;100: 2141–2151. doi:10.1007/s00253-015-7247-0
20. Scholl D, Merril C. The genome of bacteriophage K1F, a T7-like phage that has acquired the ability to replicate on K1 strains of Escherichia coli. J Bacteriol. 2005;187: 8499–8503. doi:10.1128/JB.187.24.8499-8503.2005
21. Soontarach R, Srimanote P, Enright MC, Blundell-Hunter G, Dorman MJ, Thomson NR, et al. Isolation and Characterisation of Bacteriophage Selective for Key Acinetobacter baumannii Capsule Chemotypes. Pharm Basel Switz. 2022;15: 443. doi:10.3390/ph15040443
22. Gordillo Altamirano F, Forsyth JH, Patwa R, Kostoulias X, Trim M, Subedi D, et al. Bacteriophage-resistant Acinetobacter baumannii are resensitized to antimicrobials. Nat Microbiol. 2021;6: 157–161. doi:10.1038/s41564-020-00830-7
23. JAM S, A B, M H, EPC R, O R. Modular prophage interactions driven by capsule serotype select for capsule loss under phage predation. ISME J. 2020;14: 2980–2996. doi:10.1038/s41396-020-0726-z
24. Beamud B, García-González N, Gómez-Ortega M, González-Candelas F, Domingo-Calap P, Sanjuan R. Genetic determinants of host tropism in Klebsiella phages. Cell Rep. 2023;42: 112048. doi:10.1016/j.celrep.2023.112048
25. de Sousa JAM, Buffet A, Haudiquet M, Rocha EPC, Rendueles O. Modular prophage interactions driven by capsule serotype select for capsule loss under phage predation. ISME J. 2020;14: 2980–2996. doi:10.1038/s41396-020-0726-z
26. Tan D, Zhang Y, Qin J, Le S, Gu J, Chen L, et al. A Frameshift Mutation in wcaJ Associated with Phage Resistance in Klebsiella pneumoniae. Microorganisms. 2020;8: 378. doi:10.3390/microorganisms8030378
27. Mostowy RJ, Holt KE. Diversity-Generating Machines: Genetics of Bacterial Sugar-Coating. Trends Microbiol. 2018;26: 1008–1021. doi:10.1016/j.tim.2018.06.006
28. Porter NT, Hryckowian AJ, Merrill BD, Fuentes JJ, Gardner JO, Glowacki RWP, et al. Phase-variable capsular polysaccharides and lipoproteins modify bacteriophage susceptibility in Bacteroides thetaiotaomicron. Nat Microbiol. 2020;5: 1170–1181. doi:10.1038/s41564-020-0746-5
29. Latka A, Lemire S, Grimon D, Dams D, Maciejewska B, Lu T, et al. Engineering the Modular Receptor-Binding Proteins of Klebsiella Phages Switches Their Capsule Serotype Specificity. mBio. 2021;12: e00455-21. doi:10.1128/mBio.00455-21
30. Latka A, Leiman PG, Drulis-Kawa Z, Briers Y. Modeling the Architecture of Depolymerase-Containing Receptor Binding Proteins in Klebsiella Phages. Front Microbiol. 2019;10: 2649. doi:10.3389/fmicb.2019.02649
31. Hesse S, Rajaure M, Wall E, Johnson J, Bliskovsky V, Gottesman S, et al. Phage Resistance in Multidrug-Resistant Klebsiella pneumoniae ST258 Evolves via Diverse Mutations That Culminate in Impaired Adsorption. mBio. 2020;11: e02530-19. doi:10.1128/mBio.02530-19
32. Touchon M, Moura de Sousa JA, Rocha EP. Embracing the enemy: the diversification of microbial gene repertoires by phage-mediated horizontal gene transfer. Curr Opin Microbiol. 2017;38: 66–73. doi:10.1016/j.mib.2017.04.010
33. de la Cruz F, Frost LS, Meyer RJ, Zechner EL. Conjugative DNA metabolism in Gram-negative bacteria. FEMS Microbiol Rev. 2010;34: 18–40. doi:10.1111/j.1574-6976.2009.00195.x
34. Norman A, Hansen LH, Sørensen SJ. Conjugative plasmids: vessels of the communal gene pool. Philos Trans R Soc Lond B Biol Sci. 2009;364: 2275–2289. doi:10.1098/rstb.2009.0037
35. Soucy SM, Huang J, Gogarten JP. Horizontal gene transfer: building the web of life. Nat Rev Genet. 2015;16: 472–482. doi:10.1038/nrg3962

36. León-Sampedro R, DelaFuente J, Díaz-Agero C, Crellen T, Musicha P, Rodríguez-Beltrán J, et al. Pervasive transmission of a carbapenem resistance plasmid in the gut microbiota of hospitalized patients. Nat Microbiol. 2021;6: 606–616. doi:10.1038/s41564-021-00879-y
37. Guglielmini J, Néron B, Abby SS, Garcillán-Barcia MP, de la Cruz F, Rocha EPC. Key components of the eight classes of type IV secretion systems involved in bacterial conjugation or protein secretion. Nucleic Acids Res. 2014;42: 5715–5727. doi:10.1093/nar/gku194
38. Guglielmini J, de la Cruz F, Rocha EPC. Evolution of conjugation and type IV secretion systems. Mol Biol Evol. 2013;30: 315–331. doi:10.1093/molbev/mss221
39. Lawn AM. Morphological features of the pili associated with Escherichia coli K 12 carrying R factors or the F factor. J Gen Microbiol. 1966;45: 377–383. doi:10.1099/00221287-45-2-377
40. Kishida K, Bosserman RE, Harb L, Khara P, Song L, Hu B, et al. Contributions of F-specific subunits to the F plasmid-encoded type IV secretion system and F pilus. Mol Microbiol. 2022;117: 1275–1290. doi:10.1111/mmi.14908
41. Lawley TD, Klimke WA, Gubbins MJ, Frost LS. F factor conjugation is a true type IV secretion system. FEMS Microbiol Lett. 2003;224: 1–15. doi:10.1016/S0378-1097(03)00430-0
42. Eisenbrandt R, Kalkum M, Lai EM, Lurz R, Kado CI, Lanka E. Conjugative pili of IncP plasmids, and the Ti plasmid T pilus are composed of cyclic subunits. J Biol Chem. 1999;274: 22548–22555. doi:10.1074/jbc.274.32.22548
43. Fronzes R, Christie PJ, Waksman G. The structural biology of type IV secretion systems. Nat Rev Microbiol. 2009;7: 10.1038/nrmicro2218. doi:10.1038/nrmicro2218
44. Bradley DE. Morphological and serological relationships of conjugative pili. Plasmid. 1980;4: 155–169. doi:10.1016/0147-619x(80)90005-0
45. Yong M, Chen Y, Oo G, Chang KC, Chu WHW, Teo J, et al. Dominant Carbapenemase-Encoding Plasmids in Clinical Enterobacterales Isolates and Hypervirulent Klebsiella pneumoniae, Singapore. Emerg Infect Dis. 2022;28: 1578–1588. doi:10.3201/eid2808.212542
46. Wang S, Ding Q, Zhang Y, Zhang A, Wang Q, Wang R, et al. Evolution of Virulence, Fitness, and Carbapenem Resistance Transmission in ST23 Hypervirulent Klebsiella pneumoniae with the Capsular Polysaccharide Synthesis Gene wcaJ Inserted via Insertion Sequence Elements. Microbiol Spectr. 2022; e0240022. doi:10.1128/spectrum.02400-22
47. Stuy JH. Plasmid transfer in Haemophilus influenzae. J Bacteriol. 1979;139: 520–529. doi:10.1128/JB.139.2.520-529.1979
48. Pan Y-J, Lin T-L, Chen C-T, Chen Y-Y, Hsieh P-F, Hsu C-R, et al. Genetic analysis of capsular polysaccharide synthesis gene clusters in 79 capsular types of Klebsiella spp. Sci Rep. 2015;5: 15573. doi:10.1038/srep15573
49. Heinz E, Follador R, Thomson NR, Holt KE, Kowarik M, Wyres KL, et al. The diversity of Klebsiella pneumoniae surface polysaccharides. Microb Genomics. 2016;2. doi:10.1099/mgen.0.000073
50. Wyres KL, Wick RR, Gorrie C, Jenney A, Follador R, Thomson NR, et al. Identification of Klebsiella capsule synthesis loci from whole genome data. Microb Genomics. 2016;2. doi:10.1099/mgen.0.000102
51. Ramirez MS, Traglia GM, Lin DL, Tran T, Tolmasky ME. Plasmid-Mediated Antibiotic Resistance and Virulence in Gram-Negatives: the Klebsiella pneumoniae Paradigm. Microbiol Spectr. 2014;2. doi:10.1128/microbiolspec.PLAS-0016-2013
52. Xu Y, Zhang J, Wang M, Liu M, Liu G, Qu H, et al. Mobilization of the nonconjugative virulence plasmid from hypervirulent Klebsiella pneumoniae. Genome Med. 2021;13: 119. doi:10.1186/s13073-021-00936-5
53. Navon-Venezia S, Kondratyeva K, Carattoli A. Klebsiella pneumoniae: a major worldwide source and shuttle for antibiotic resistance. FEMS Microbiol Rev. 2017;41: 252–275. doi:10.1093/femsre/fux013

54. DelaFuente J, Toribio-Celestino L, Santos-Lopez A, León-Sampedro R, Alonso-Del Valle A, Costas C, et al. Within-patient evolution of plasmid-mediated antimicrobial resistance. Nat Ecol Evol. 2022;6: 1980–1991. doi:10.1038/s41559-022-01908-7
55. Wyres KL, Lam MMC, Holt KE. Population genomics of Klebsiella pneumoniae. Nat Rev Microbiol. 2020;18: 344–359. doi:10.1038/s41579-019-0315-1
56. Thorpe HA, Booton R, Kallonen T, Gibbon MJ, Couto N, Passet V, et al. A large-scale genomic snapshot of Klebsiella spp. isolates in Northern Italy reveals limited transmission between clinical and non-clinical settings. Nat Microbiol. 2022;7: 2054–2067. doi:10.1038/s41564-022-01263-0
57. Kortright KE, Chan BK, Koff JL, Turner PE. Phage Therapy: A Renewed Approach to Combat Antibiotic-Resistant Bacteria. Cell Host Microbe. 2019;25: 219–232. doi:10.1016/j.chom.2019.01.014
58. Yu W-L, Ko W-C, Cheng K-C, Lee C-C, Lai C-C, Chuang Y-C. Comparison of prevalence of virulence factors for Klebsiella pneumoniae liver abscesses between isolates with capsular K1/K2 and non-K1/K2 serotypes. Diagn Microbiol Infect Dis. 2008;62. doi:10.1016/j.diagmicrobio.2008.04.007
59. Yeh K-M, Kurup A, Siu LK, Koh YL, Fung C-P, Lin J-C, et al. Capsular serotype K1 or K2, rather than magA and rmpA, is a major virulence determinant for Klebsiella pneumoniae liver abscess in Singapore and Taiwan. J Clin Microbiol. 2007;45: 466–471. doi:10.1128/JCM.01150-06
60. David S, Reuter S, Harris G SR, C F, T A, S. Epidemic of carbapenem-resistant Klebsiella pneumoniae in Europe is driven by nosocomial spread. Nat Microbiol. 2019;4: 1919–1929. doi:10.1038/s41564-019-0492-8
61. Corelli B, Almeida AS, Sonego F, Castiglia V, Fevre C, Brisse S. Rhinoscleroma pathogenesis: The type K3 capsule of Klebsiella rhinoscleromatis is a virulence factor not involved in Mikulicz cells formation. PLoS Negl Trop Dis. 2018;12: 0006201. doi:10.1371/journal.pntd.0006201
62. Lam MMC, Wick RR, Wyres KL, Gorrie CL, Judd LM, Jenney AWJ, et al. Genetic diversity, mobilisation and spread of the yersiniabactin-encoding mobile element ICEKp in Klebsiella pneumoniae populations. Microb Genomics. 2018;4: e000196. doi:10.1099/mgen.0.000196
63. Beamud B, García-González N, Gómez-Ortega M, González-Candelas F, Domingo-Calap P, Sanjuan R. Genetic determinants of host tropism in Klebsiella phages. bioRxiv; 2022. p. 2022.06.01.494021. doi:10.1101/2022.06.01.494021
64. Pfeifer E, Sousa JM, Touchon M, Rocha EP. When bacteria are phage playgrounds: interactions between viruses, cells, and mobile genetic elements. Curr Opin Microbiol. 2022;70: 102230. doi:10.1016/j.mib.2022.102230
65. Haudiquet M, de Sousa JM, Touchon M, Rocha EPC. Selfish, promiscuous and sometimes useful: how mobile genetic elements drive horizontal gene transfer in microbial populations. Philos Trans R Soc Lond B Biol Sci. 2022;377: 20210234. doi:10.1098/rstb.2021.0234
66. Tesson F, Hervé A, Mordret E, Touchon M, d'Humières C, Cury J, et al. Systematic and quantitative view of the antiviral arsenal of prokaryotes. Nat Commun. 2022;13: 2561. doi:10.1038/s41467-022-30269-9
67. Abby SS, Néron B, Ménager H, Touchon M, Rocha EPC. MacSyFinder: a program to mine genomes for molecular systems with an application to CRISPR-Cas systems. PloS One. 2014;9: e110726. doi:10.1371/journal.pone.0110726
68. Piel D, Bruto M, Labreuche Y, Blanquart F, Goudenège D, Barcia-Cruz R, et al. Phage-host coevolution in natural populations. Nat Microbiol. 2022;7: 1075–1086. doi:10.1038/s41564-022-01157-1

69. Patro LPP, Sudhakar KU, Rathinavelan T. K-PAM: a unified platform to distinguish Klebsiella species K- and O-antigen types, model antigen structures and identify hypervirulent strains. Sci Rep. 2020;10: 16732. doi:10.1038/s41598-020-73360-1
70. Tesson F, Hervé A, Mordret E, Touchon M, d'Humières C, Cury J. Systematic and quantitative view of the antiviral arsenal of prokaryotes. Nat Commun. 2022;13: 2561. doi:10.1038/s41467-022-30269-9
71. Low WW, Wong JLC, Beltran LC, Seddon C, David S, Kwong H-S, et al. Mating pair stabilization mediates bacterial conjugation species specificity. Nat Microbiol. 2022;7: 1016–1027. doi:10.1038/s41564-022-01146-4
72. Huisman JS, Benz F, Duxbury SJN, de Visser JAGM, Hall AR, Fischer EAJ, et al. Estimating plasmid conjugation rates: A new computational tool and a critical comparison of methods. Plasmid. 2022;121: 102627. doi:10.1016/j.plasmid.2022.102627
73. Zhong X, Droesch J, Fox R, Top EM, Krone SM. On the meaning and estimation of plasmid transfer rates for surface-associated and well-mixed bacterial populations. J Theor Biol. 2012;294: 144–152. doi:10.1016/j.jtbi.2011.10.034
74. Stuy JH. Plasmid transfer in Haemophilus influenzae. J Bacteriol. 1979;139: 520–529. doi:10.1128/JB.139.2.520-529.1979
75. Shao X, Mugler A, Kim J, Jeong HJ, Levin BR, Nemenman I. Growth of bacteria in 3-d colonies. PLoS Comput Biol. 2017;13: 1005679. doi:10.1371/journal.pcbi.1005679
76. Buffet A, Rocha EPC, Rendueles O. Nutrient conditions are primary drivers of bacterial capsule maintenance in Klebsiella. Proc Biol Sci. 2021;288: 20202876. doi:10.1098/rspb.2020.2876
77. Walker KA, Miller VL. The intersection of capsule gene expression, hypermucoviscosity and hypervirulence in Klebsiella pneumoniae. Curr Opin Microbiol. 2020;54: 95–102. doi:10.1016/j.mib.2020.01.006
78. Doron S, Melamed S, Ofir G, Leavitt A, Lopatina A, Keren M, et al. Systematic discovery of antiphage defense systems in the microbial pangenome. Science. 2018;359: eaar4120. doi:10.1126/science.aar4120
79. Achtman M, Kennedy N, Skurray R. Cell--cell interactions in conjugating Escherichia coli: role of traT protein in surface exclusion. Proc Natl Acad Sci U S A. 1977;74: 5104–5108. doi:10.1073/pnas.74.11.5104
80. Vulić M, Dionisio F, Taddei F, Radman M. Molecular keys to speciation: DNA polymorphism and the control of genetic exchange in enterobacteria. Proc Natl Acad Sci U S A. 1997;94: 9763–9767. doi:10.1073/pnas.94.18.9763
81. Whitfield C, Williams DM, Kelly SD. Lipopolysaccharide O-antigens—bacterial glycans made to measure. J Biol Chem. 2020;295: 10593–10609. doi:10.1074/jbc.REV120.009402
82. Hathaway LJ, Brugger SD, Morand B, Bangert M, Rotzetter JU, Hauser C, et al. Capsule type of Streptococcus pneumoniae determines growth phenotype. PLoS Pathog. 2012;8: e1002574. doi:10.1371/journal.ppat.1002574
83. Croucher NJ, Kagedan L, Thompson CM, Parkhill J, Bentley SD, Finkelstein JA. Selective and Genetic Constraints on Pneumococcal Serotype Switching. PLoS Genet. 2015;11: e1005095. doi:10.1371/journal.pgen.1005095
84. Alcalá B, Arreaza L, Salcedo C, Uría MJ, De La Fuente L, Vázquez JA. Capsule switching among C:2b:P1.2,5 meningococcal epidemic strains after mass immunization campaign, Spain. Emerg Infect Dis. 2002;8: 1512–1514. doi:10.3201/eid0812.020081
85. Scholl D, Adhya S, Merril C. Escherichia coli K1's capsule is a barrier to bacteriophage T7. Appl Env Microbiol. 2005;71: 4872–4874. doi:10.1128/AEM.71.8.4872-4874.2005
86. Soundararajan M, Bünau R, Oelschlaeger TA. K5 Capsule and Lipopolysaccharide Are Important in Resistance to T4 Phage Attack in Probiotic E. coli Strain Nissle 1917. Front Microbiol. 2019;10: 2783. doi:10.3389/fmicb.2019.02783

87. Wilkinson BJ, Holmes KM. Staphylococcus aureus cell surface: capsule as a barrier to bacteriophage adsorption. Infect Immun. 1979;23: 549–552.
88. Matilla MA, Salmond GPC. Bacteriophage ϕMAM1, a viunalikevirus, is a broad-host-range, high-efficiency generalized transducer that infects environmental and clinical isolates of the enterobacterial genera Serratia and Kluyvera. Appl Environ Microbiol. 2014;80: 6446–6457. doi:10.1128/AEM.01546-14
89. Soontarach R, Srimanote P, Enright MC, Blundell-Hunter G, Dorman MJ, Thomson NR. Isolation and Characterisation of Bacteriophage Selective for Key Acinetobacter baumannii Capsule Chemotypes. Pharm Basel Switz. 2022;15: 443. doi:10.3390/ph15040443
90. Rieger-Hug D, Stirm S. Comparative study of host capsule depolymerases associated with Klebsiella bacteriophages. Virology. 1981;113: 363–378. doi:10.1016/0042-6822(81)90162-8
91. Pires DP, Oliveira H, Melo LDR, Sillankorva S, Azeredo J. Bacteriophage-encoded depolymerases: their diversity and biotechnological applications. Appl Microbiol Biotechnol. 2016;100: 2141–2151. doi:10.1007/s00253-015-7247-0
92. Latka A, Leiman PG, Drulis-Kawa Z, Briers Y. Modeling the Architecture of Depolymerase-Containing Receptor Binding Proteins in Klebsiella Phages. Front Microbiol. 2019;10: 2649. doi:10.3389/fmicb.2019.02649
93. Bayer ME, Thurow H, Bayer MH. Penetration of the polysaccharide capsule of Escherichia coli (Bi161/42) by bacteriophage K29. Virology. 1979;94: 95–118. doi:10.1016/0042-6822(79)90441-0
94. Valle AA, Toribio-Celestino L, Quirant A, Pi CT, DelaFuente J, Canton R, et al. Differences in vertical and horizontal transmission dynamics shape plasmid distribution in clinical enterobacteria. bioRxiv; 2023. p. 2023.04.03.535338. doi:10.1101/2023.04.03.535338
95. Wanford JJ, Hames RG, Carreno D, Jasiunaite Z, Chung WY, Arena F, et al. Interaction of Klebsiella pneumoniae with tissue macrophages in a mouse infection model and ex-vivo pig organ perfusions: an exploratory investigation. Lancet Microbe. 2021;2: e695–e703. doi:10.1016/S2666-5247(21)00195-6
96. Struve C, Roe CC, Stegger M, Stahlhut SG, Hansen DS, Engelthaler DM, et al. Mapping the Evolution of Hypervirulent Klebsiella pneumoniae. mBio. 2015;6: e00630. doi:10.1128/mBio.00630-15
97. Kostina E, Ofek I, Crouch E, Friedman R, Sirota L, Klinger G. Noncapsulated Klebsiella pneumoniae bearing mannose-containing O antigens is rapidly eradicated from mouse lung and triggers cytokine production by macrophages following opsonization with surfactant protein D. Infect Immun. 2005;73: 8282–8290. doi:10.1128/IAI.73.12.8282-8290.2005
98. Wu M-F, Yang C-Y, Lin T-L, Wang J-T, Yang F-L, Wu S-H, et al. Humoral Immunity against Capsule Polysaccharide Protects the Host from magA+ Klebsiella pneumoniae-Induced Lethal Disease by Evading Toll-Like Receptor 4 Signaling. Infect Immun. 2009;77: 615–621. doi:10.1128/IAI.00931-08
99. Lan P, Jiang Y, Zhou J, Yu Y. A global perspective on the convergence of hypervirulence and carbapenem resistance in Klebsiella pneumoniae. J Glob Antimicrob Resist. 2021;25: 26–34. doi:10.1016/j.jgar.2021.02.020
100. Granato ET, Meiller-Legrand TA, Foster KR. The Evolution and Ecology of Bacterial Warfare. Curr Biol CB. 2019;29: R521–R537. doi:10.1016/j.cub.2019.04.024
101. Wallden K, Rivera-Calzada A, Waksman G. Type IV secretion systems: versatility and diversity in function. Cell Microbiol. 2010;12: 1203–1212. doi:10.1111/j.1462-5822.2010.01499.x
102. Souza DP, Oka GU, Alvarez-Martinez CE, Bisson-Filho AW, Dunger G, Hobeika L, et al. Bacterial killing via a type IV secretion system. Nat Commun. 2015;6: 6453. doi:10.1038/ncomms7453
103. Hauser AR. The Type III Secretion System of Pseudomonas aeruginosa: Infection by Injection. Nat Rev Microbiol. 2009;7: 654–665. doi:10.1038/nrmicro2199

104. Basler M. Type VI secretion system: secretion by a contractile nanomachine. Philos Trans R Soc Lond B Biol Sci. 2015;370: 20150021. doi:10.1098/rstb.2015.0021
105. Coulthurst S. The Type VI secretion system: a versatile bacterial weapon. Microbiol Read Engl. 2019;165: 503–515. doi:10.1099/mic.0.000789
106. Flaugnatti N, Isaac S, Lemos Rocha LF, Stutzmann S, Rendueles O, Stoudmann C, et al. Human commensal gut Proteobacteria withstand type VI secretion attacks through immunity protein-independent mechanisms. Nat Commun. 2021;12: 5751. doi:10.1038/s41467-021-26041-0
107. Hersch SJ, Watanabe N, Stietz MS, Manera K, Kamal F, Burkinshaw B, et al. Envelope stress responses defend against type six secretion system attacks independently of immunity proteins. Nat Microbiol. 2020;5: 706–714. doi:10.1038/s41564-020-0672-6
108. Geller AM, Pollin I, Zlotkin D, Danov A, Nachmias N, Andreopoulos WB, et al. The extracellular contractile injection system is enriched in environmental microbes and associates with numerous toxins. Nat Commun. 2021;12: 3743. doi:10.1038/s41467-021-23777-7
109. Köhler T, Donner V, van Delden C. Lipopolysaccharide as Shield and Receptor for R-Pyocin-Mediated Killing in Pseudomonas aeruginosa. J Bacteriol. 2010;192: 1921–1928. doi:10.1128/JB.01459-09
110. Kuhlman TE, Cox EC. Site-specific chromosomal integration of large synthetic constructs. Nucleic Acids Res. 2010;38: e92. doi:10.1093/nar/gkp1193
111. Deatherage DE, Barrick JE. Identification of mutations in laboratory evolved microbes from next-generation sequencing data using breseq. Methods Mol Biol Clifton NJ. 2014;1151: 165–188. doi:10.1007/978-1-4939-0554-6_12
112. Lin T-L, Hsieh P-F, Huang Y-T, Lee W-C, Tsai Y-T, Su P-A, et al. Isolation of a bacteriophage and its depolymerase specific for K1 capsule of Klebsiella pneumoniae: implication in typing and treatment. J Infect Dis. 2014;210: 1734–1744. doi:10.1093/infdis/jiu332
113. Carattoli A, Zankari E, García-Fernández A, Voldby Larsen M, Lund O, Villa L, et al. In Silico Detection and Typing of Plasmids using PlasmidFinder and Plasmid Multilocus Sequence Typing. Antimicrob Agents Chemother. 2014;58: 3895–3903. doi:10.1128/AAC.02412-14
114. Cury J, Abby SS, Doppelt-Azeroual O, Néron B, Rocha EPC. Identifying Conjugative Plasmids and Integrative Conjugative Elements with CONJscan. Methods Mol Biol Clifton NJ. 2020;2075: 265–283. doi:10.1007/978-1-4939-9877-7_19
115. Bortolaia V, Kaas RS, Ruppe E, Roberts MC, Schwarz S, Cattoir V, et al. ResFinder 4.0 for predictions of phenotypes from genotypes. J Antimicrob Chemother. 2020;75: 3491–3500. doi:10.1093/jac/dkaa345
116. Ghigo JM. Natural conjugative plasmids induce bacterial biofilm development. Nature. 2001;412: 442–445. doi:10.1038/35086581
117. Abby SS, Rocha EPC. Identification of Protein Secretion Systems in Bacterial Genomes Using MacSyFinder. Methods Mol Biol. 2017;1615: 1–21. doi:10.1007/978-1-4939-7033-9_1
118. Lam MMC, Wick RR, Watts SC, Cerdeira LT, Wyres KL, Holt KE. A genomic surveillance framework and genotyping tool for Klebsiella pneumoniae and its related species complex. Nat Commun. 2021;12: 4188. doi:10.1038/s41467-021-24448-3
119. Camacho C, Coulouris G, Avagyan V, Ma N, Papadopoulos J, Bealer K, et al. BLAST+: architecture and applications. BMC Bioinformatics. 2009;10: 421. doi:10.1186/1471-2105-10-421
120. Pitcher DG, Saunders NA, Owen RJ. Rapid extraction of bacterial genomic DNA with guanidium thiocyanate. Lett Appl Microbiol. 1989;8: 151–156. doi:10.1111/j.1472-765X.1989.tb00262.x
121. Prjibelski A, Antipov D, Meleshko D, Lapidus A, Korobeynikov A. Using SPAdes De Novo Assembler. Curr Protoc Bioinforma. 2020;70: e102. doi:10.1002/cpbi.102
122. Wyres KL, Wick RR, Gorrie C, Jenney A, Follador R, Thomson NR, et al. Identification of Klebsiella capsule synthesis loci from whole genome data. Microb Genomics. 2016;2: e000102. doi:10.1099/mgen.0.000102

123. Rice P, Longden I, Bleasby A. EMBOSS: the European Molecular Biology Open Software Suite. Trends Genet TIG. 2000;16: 276–277. doi:10.1016/s0168-9525(00)02024-2
124. Li H. Aligning sequence reads, clone sequences and assembly contigs with BWA-MEM. arXiv; 2013. doi:10.48550/ARXIV.1303.3997
125. Robinson JT, Thorvaldsdóttir H, Winckler W, Guttman M, Lander ES, Getz G, et al. Integrative Genomics Viewer. Nat Biotechnol. 2011;29: 24–26. doi:10.1038/nbt.1754
126. Buffet A, Rocha EPC, Rendueles O. Nutrient conditions are primary drivers of bacterial capsule maintenance in Klebsiella. Proc Biol Sci. 2021;288: 20202876. doi:10.1098/rspb.2020.2876
127. Levin BR, Stewart FM, Rice VA. The kinetics of conjugative plasmid transmission: Fit of a simple mass action model. Plasmid. 1979;2: 247–260. doi:10.1016/0147-619X(79)90043-X
128. Lopatkin AJ, Huang S, Smith RP, Srimani JK, Sysoeva TA, Bewick S, et al. Antibiotics as a selective driver for conjugation dynamics. Nat Microbiol. 2016;1: 16044. doi:10.1038/nmicrobiol.2016.44
129. Ondov BD, Treangen TJ, Melsted P, Mallonee AB, Bergman NH, Koren S, et al. Mash: fast genome and metagenome distance estimation using MinHash. Genome Biol. 2016;17: 132. doi:10.1186/s13059-016-0997-x
130. Perrin A, Rocha EPC. PanACoTA: a modular tool for massive microbial comparative genomics. NAR Genomics Bioinforma. 2021;3: lqaa106. doi:10.1093/nargab/lqaa106
131. Kalyaanamoorthy S, Minh BQ, Wong TKF, von Haeseler A, Jermiin LS. ModelFinder: fast model selection for accurate phylogenetic estimates. Nat Methods. 2017;14: 587–589. doi:10.1038/nmeth.4285
132. Hoang DT, Chernomor O, von Haeseler A, Minh BQ, Vinh LS. UFBoot2: Improving the Ultrafast Bootstrap Approximation. Mol Biol Evol. 2018;35: 518–522. doi:10.1093/molbev/msx281
133. Schliep KP. phangorn: phylogenetic analysis in R. Bioinformatics. 2011;27: 592–593. doi:10.1093/bioinformatics/btq706
134. Lam MMC, Wick RR, Judd LM, Holt KE, Wyres KL. Kaptive 2.0: updated capsule and lipopolysaccharide locus typing for the Klebsiella pneumoniae species complex. Microb Genomics. 2022;8. doi:10.1099/mgen.0.000800
135. Ishikawa SA, Zhukova A, Iwasaki W, Gascuel O. A Fast Likelihood Method to Reconstruct and Visualize Ancestral Scenarios. Mol Biol Evol. 2019;36: 2069–2085. doi:10.1093/molbev/msz131
136. Fox J, Weisberg S. An R Companion to Applied Regression. Third. Thousand Oaks CA: Sage; 2019. Available: https://socialsciences.mcmaster.ca/jfox/Books/Companion/
137. Wickham H, Averick M, Bryan J, Chang W, McGowan LD, François R, et al. Welcome to the Tidyverse. J Open Source Softw. 2019;4: 1686. doi:10.21105/joss.01686
138. Paradis E, Claude J, Strimmer K. APE: Analyses of Phylogenetics and Evolution in R language. Bioinforma Oxf Engl. 2004;20: 289–290. doi:10.1093/bioinformatics/btg412
139. Wang L-G, Lam TT-Y, Xu S, Dai Z, Zhou L, Feng T, et al. Treeio: An R Package for Phylogenetic Tree Input and Output with Richly Annotated and Associated Data. Mol Biol Evol. 2020;37: 599–603. doi:10.1093/molbev/msz240